AD-A130 764 CHARACTERIZATION OF P-TYPE CDTE ELECTRODES IN ACETONITRILE/ELECTROLYTE SO..(U) MASSACHUSETTS INST OF TECH CAMBRIDGE DEPT OF CHEMISTRY H S WHITE ET AL. 1/1

UNCLASSIFIED 30 JUN 83 TR-39-ONR N00014-75-C-0880 F/G 9/1 NL

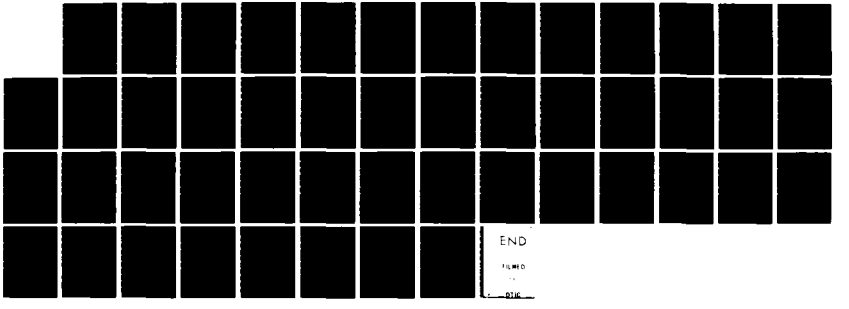

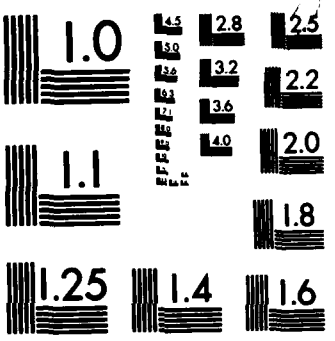

UNCLASSIFIED

SECURITY CLASSIFICATION OF THIS PAGE (When Data Entered)

(12)

REPORT DOCUMENTATION PAGE

READ INSTRUCTIONS BEFORE COMPLETING FORM

1. REPORT NUMBER: ONR-TR-39	2. GOVT ACCESSION NO.: AD-A130 764
3. RECIPIENT'S CATALOG NUMBER:	
4. TITLE (and Subtitle): "Characterization of p-Type CdTe Electrodes in Acetonitrile/Electrolyte Solutions. Nearly Ideal Behavior from Reductive Surface Pretreatments."	5. TYPE OF REPORT & PERIOD COVERED: Interim Technical Report
	6. PERFORMING ORG. REPORT NUMBER:
7. AUTHOR(s): Henry S. White, Antonio J. Ricco and Mark S. Wrighton	8. CONTRACT OR GRANT NUMBER(s): N00014-75-C-0880
9. PERFORMING ORGANIZATION NAME AND ADDRESS: Department of Chemistry, Rm. 6-335, Massachusetts Institute of Technology, Cambridge, Massachusetts 02139	10. PROGRAM ELEMENT, PROJECT, TASK AREA & WORK UNIT NUMBERS: NR 051-579
11. CONTROLLING OFFICE NAME AND ADDRESS: Office of Naval Research, Department of the Navy, Arlington, Virginia 22215	12. REPORT DATE: June 30, 1983 13. NUMBER OF PAGES: 49
14. MONITORING AGENCY NAME & ADDRESS (if different from Controlling Office)	15. SECURITY CLASS. (of this report): Unclassified 15a. DECLASSIFICATION/DOWNGRADING SCHEDULE

16. DISTRIBUTION STATEMENT (of this Report)

Approved for public release; reproduction is permitted for any purpose of the United States Government; distribution unlimited.

17. DISTRIBUTION STATEMENT (of the abstract entered in Block 20, if different from Report)

Distribution of this document is unlimited.

18. SUPPLEMENTARY NOTES

Prepared for publication in the Journal of the American Chemical Society.

19. KEY WORDS (Continue on reverse side if necessary and identify by block number)

characterization, cadmium telluride, surfaces, etching, electrodes

20. ABSTRACT (Continue on reverse side if necessary and identify by block number)

See reverse for Abstract.

DD FORM 1 JAN 73 1473 EDITION OF 1 NOV 65 IS OBSOLETE S/N 0102-014-6601

UNCLASSIFIED

SECURITY CLASSIFICATION OF THIS PAGE (When Data Entered)

OFFICE OF NAVAL RESEARCH

CONTRACT N00014-75-C-0880

Task No. NR 051-579

TECHNICAL REPORT NO. 39

"CHARACTERIZATION OF p-TYPE CdTe ELECTRODES IN ACETONITRILE/ELECTROLYTE SOLUTIONS. NEARLY IDEAL BEHAVIOR FROM REDUCTIVE SURFACE PRETREATMENTS"

by

Henry S. White, Antonio J. Ricco and Mark S. Wrighton

Department of Chemistry
Massachusetts Institute of Technology
Cambridge, Massachusetts 02139

Prepared for publication in the Journal of the American Chemical Society

June 30, 1983

Abstract

Single crystal p-CdTe (E_g = 1.4 eV) electrodes have been characterized in CH_3CN/electrolyte solutions. Deliberate modification of the p-CdTe surface by etching in strongly oxidizing ($Cr_2O_7^{2-}/HNO_3$) or reducing ($S_2O_4^{2-}/OH^-$) solutions alters the p-CdTe surface to give rise to large differences in the electrochemical response in the dark and under illumination. The oxidative pretreatment apparently yields a p-CdTe surface that is Fermi level pinned, whereas the reductive pretreatment yields nearly ideal response. The pretreated electrodes were characterized by XPS, impedance measurements, and cyclic voltammetry in the presence of a number of reversible, one-electron redox couples. XPS indicates the presence of a Te-rich surface overlayer, composed of Te^0 and TeO_2, on CdTe etched in oxidizing media. Electrodes etched in reducing solutions yield XPS spectra nearly identical to those of an Ar ion-sputtered CdTe sample, in terms of stoichiometry (1:1) and chemical state (Cd^{2+} and Te^{2-}) of cadmium and telluride. The differential capacitance of p-CdTe cathodes in CH_3CN/0.2 M $[n\text{-}Bu_4N]BF_4$ was measured in the dark over the potential range -0.2 to -1.0 V vs. SSCE. Linear Mott-Schottky plots (E_{FB} = -0.4 V vs. SSCE, n_A = 2.5 x 10^{15} cm^{-3}) are obtained for electrodes etched in $S_2O_4^{2-}/OH^-$ solutions consistent with ideal variation in the band bending as the electrode potential is varied. In contrast, p-CdTe etched in $Cr_2O_7^{2-}/HNO_3$ yields potential-independent values of differential capacitance, ~40-70 $nF \cdot cm^{-2}$, consistent with constant band bending (<0.1 eV) over a wide potential range. Quasi-reversible cyclic voltammetry in the dark and negligible photovoltages under illumination are observed at p-CdTe electrodes pretreated with the oxidative etch, consistent with the small barrier height determined from capacitance measurements. The CdTe etched in $S_2O_4^{2-}/OH^-$ solution shows nearly ideal interfacial behavior. Photovoltages vary from 0.0 to 0.7 V for solution species having redox potentials from -0.4 to -2.0 V vs. SSCE. The sustained conversion of 632.8 nm light (~40 mW/cm^2) to electricity has been demonstrated to be ~8% efficient for a solution containing [1,2-dicyanobenzene]$^{0/-}$. The cell has an open-circuit photovoltage of up to 0.9 V, a short-circuit quantum yield for electron flow of ~0.5 and a fill factor of ~0.45.

Characterization of p-Type CdTe Electrodes in Acetonitrile/Electrolyte Solutions. Nearly Ideal Behavior From Reductive Surface Pretreatments

Henry S. White, Antonio J. Ricco, and Mark S. Wrighton*

Department of Chemistry
Massachusetts Institute of Technology
Cambridge, Massachusetts 02139

A

*Address correspondence to this author.

An earlier report from this laboratory[1] demonstrated the ability to alter and control the photoelectrochemical response of n-type semiconducting CdTe by deliberate modification of the electrode surface. Specifically, the photovoltage, E_V, developed at CdTe photoanodes pretreated by chemical etching in strongly oxidizing solutions is found to be insensitive to the solution redox potential,[1,2] E_{redox}, over a large potential range. In contrast, electrodes etched by a reducing solution behave in an ideal fashion:[3] the observed E_V was found to increase linearly with more oxidizing solution potentials. We and others[1,2,4,5] generally assume that the maximum photovoltage, $E_V(max)$, observed at a semiconductor electrode under illumination corresponds closely to the barrier height, E_B, associated with the semiconductor/liquid electrolyte junction at equilibrium in the dark, equation (1) and Scheme I. Thus, the constant photovoltage

$$E_B \cong E_V(max) \qquad (1)$$

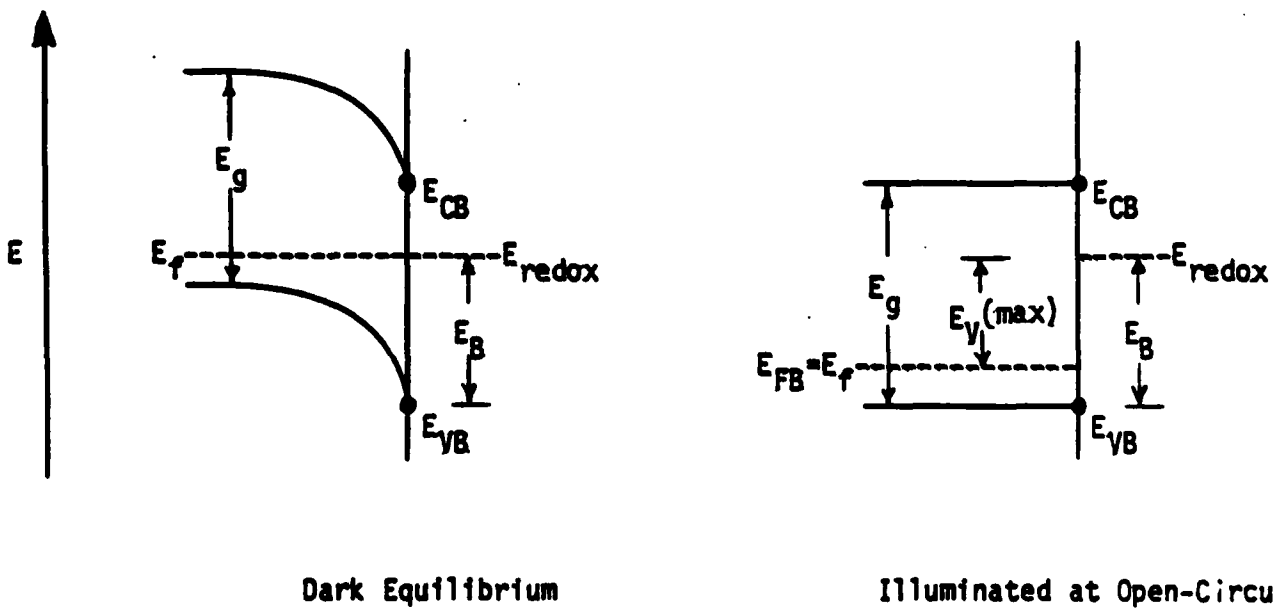

Dark Equilibrium

Illuminated at Open-Circuit

Scheme I: Interface energetics from a p-type semiconductor in contact with an electrolyte/redox couple/solvent system in the dark at equilibrium and under illumination with intense, $>E_g$ light at open-circuit.

observed at "surface oxidized" n-CdTe electrodes indicates a constant barrier height, independent of the solution potential.[1] This situation is observed at small bandgap semiconductors[6] in contact with electrolytic solutions or metal over-layers and is referred to as "Fermi level pinning".[6] Fermi level pinning is associated with a high density of surface states located between the conduction and valence band edges E_{CB} and E_{VB}. Depending on the density and distribution of surface states, the charging of the surface states by equilibration of the surface with redox species in solution or with the bulk of the semiconductor can result in a constant amount of band bending, independent of E_{redox}. In such cases variation in E_{redox} results in variation in the potential drop across the electrode/electrolyte interface (Helmholtz layer) and not across the semiconductor to cause changes in band bending. The large variation of photovoltage with E_{redox} observed at "surface reduced" n-type CdTe[1] leads to the conclusion that these surface energy levels can be removed by chemical methods, resulting in a more ideal CdTe semiconductor/liquid electrolyte junction.

We now wish to report the results of a related investigation concerning the influence of chemical pretreatment on the behavior of p-type CdTe in contact with CH_3CN/electrolyte solutions. In contrast to n-type cadmium chalcogenides,[7-10] CdX (X = S, Se, and Te), p-CdTe has been relatively unexplored as an electrode in photoelectrochemical cells. This is probably due, in part, to the poor performance found ($E_V(max) < 100$ mV) in the few investigations.[11] We point out, however, that CdTe is one of the few II-VI compounds that can be made even moderately p-type [12] and that its band gap, E_g, of 1.4 eV[13] corresponds to the optimum value for solar energy conversion.[14] Studies of p-CdTe/metal Schottky barriers have shown that it is possible to obtain relatively large values of E_B, but values of $E_V(max)$ have apparently not been measured.[15] In view of the

previous success from surface modification in altering the behavior of n-CdTe,[1] we felt that a similar strategy applied to p-type CdTe might result in an increase in its output performance. It is demonstrated that p-CdTe electrodes pretreated using a reducing etchant behave in a nearly ideal fashion with photovoltages varying from negligible values up to 0.9 V, depending on E_{redox}. In addition to measuring the photovoltage developed at illuminated electrodes, independent measurements of the barrier heights, E_B, of both oxidized and reduced p-type and n-type CdTe have been obtained from differential capacitance measurements. The values of E_B determined from capacitance studies correspond closely to the measured values of photovoltage (E_V) of these materials, supporting the assumption given in equation (1).

Experimental

Electrode Fabrication. Single crystals of p- and n-CdTe (Cleveland Crystals, Cleveland, OH) were cut into 0.05-0.2 cm^2 wafers approximately 1-2 mm thick. Before fabricating the crystals into electrodes, the side of the crystal to be exposed to the electrolyte solution was polished to a mirror finish with 0.3 μm alumina. Ohmic contact to n-CdTe was then made by rubbing In-Ga eutectic onto the back side of the crystal. Ohmic contact to p-CdTe was made by a slight modification of a procedure previously described by Aven and Garwacki for making ohmic contacts to p-ZnTe.[16] After polishing the face to be exposed to solution, the crystal was etched in boiling 5 M KOH for 1 minute, rinsed thoroughly with H_2O and dried. Approximately 20 $\mu l/cm^2$ of a 0.1 M $LiNO_3$ solution was applied to the back side of the crystal and allowed to evaporate to dryness under an Ar atmosphere. The p-CdTe crystal was then heated slowly to 400°C under a H_2-N_2 atmosphere (10% H_2) and held at this temperature for 1 h. Under these conditions Li is reported to diffuse slowly into the crystal. After cooling to room temperature, the crystal was rinsed with H_2O to remove excess $LiNO_3$, and a gold electroless contact was plated onto the Li diffused area with $HAuCl_4$. Excess plating solution was removed from the back surface with tissue and the contact was dried at 100°C for ca. 2 minutes. A Cu wire was then attached to the ohmic contacts of both n- and p-CdTe using Ag conductive paint and the entire assembly was mounted in glass tubing with ordinary epoxy leaving only the front crystal face, <111> orientation, exposed as previously described.[1]

Etching Procedure. CdTe electrodes were etched in reducing or oxidizing solutions immediately prior to their use. The oxidizing etch consisted of a 30 s immersion of the electrode in a solution containing 4 g $K_2Cr_2O_7$, 10 ml conc. HNO_3 and 20 ml H_2O. For the reducing etch, the electrode surface was initially

oxidized in the above etchant, then immersed for 3 min in a boiling solution of 0.6 M $Na_2S_2O_4$ and 2.5 M NaOH. After each etching the electrode was rinsed thoroughly with distilled H_2O, then acetone. Prolonged or repeated etching of CdTe electrodes resulted in a surface that appeared roughened; such electrodes showed poor, irreproducible electrochemical behavior and therefore were not employed until the surface had been repolished.

Electrochemical Procedure and Apparatus. Electrochemical measurements were made in a single compartment cell (~40 ml) equipped with an optically flat Pyrex® window. Cyclic voltammetry was performed in Ar- or N_2-purged CH_3CN solutions containing 0.2 M [n-Bu_4N]BF_4 as supporting electrolyte. The redox reagent concentration was typically 1-3 mM except where noted otherwise. Along with the semiconductor electrode, the cell contained a Pt disk electrode to check electrolyte and reagent purity, an 8 cm^2 Pt foil counterelectrode, and an aqueous sodium-saturated calomel reference electrode (SSCE). All potentials are reported vs. SSCE, which is 52 mV negative of the SCE (saturated calomel electrode).[17] Cyclic voltammograms were measured with a Pine Instruments Model RDE3 potentiostat/programmer and recorded on a Houston Instruments Model 2000 X-Y recorder.

Differential capacitance measurements were made under the conditions described above employing a Princeton Applied Research Model 5204 lock-in amplifier with internal oscillator. Differential capacitance was recorded as a function of applied potential by scanning the d.c. potential at 5 mV/sec. A ~10 mV peak-to-peak sine wave, 100 Hz-3 kHz, was used to modulate the electrode potential. Capacitance values were extracted from the quadrature values by assuming a simple RC series circuit. A dummy RC circuit was used to calibrate the measuring system. Quadrature readings were insensitive to R over the range

100-800 Ω, indicating a strict proportionality of the quadrature output to the actual capacitance value.

The light source used to irradiate the photoelectrodes was a beam expanded 5 mW He-Ne laser (632.8 nm). Intensities were varied with a beam expander or by neutral density filters. A Tektronix J16 radiometer equipped with a J6502 probe was used to measure the input 632.8 nm optical power.

Photoaction Spectroscopy. Photoaction spectra were obtained by interfacing a PAR Model 6001 photoacoustic spectrometer with a potentiostat. The photoacoustic sample cell was replaced by a single compartment three-electrode electrochemical cell with CdTe photoelectrode positioned in the light beam. While maintaining the photoelectrode on the plateau of the appropriate current-voltage curve, the wavelength was scanned and the output of the potentiostat sent to the Model 6001's microprocessor. A beam splitter and pyroelectric detector provided correction for variation in light intensity with wavelength, hence division of the resulting photocurrent spectra by a signal proportional to wavelength yielded relative quantum yield spectra. A 1 kW Xe arc lamp, modulated at 100 Hz, provided 10-100 mW/cm^2 of monochromatic visible light (8 nm resolution) to the photoelectrode. Lock-in detection eliminated dark current.

Surface Spectroscopy. X-ray photoelectron spectra were recorded on a PDP 11/04-controlled Physical Electronics (Perkin Elmer) Model 548 spectrometer[18] equipped with Mg anode and cylindrical mirror analyzer (CMA). Spectra were recorded in digital format using a 0.5 eV step size and 100 eV pass energy for survey scans (1000-0 eV), and a 0.2 eV step size and 25 eV pass energy for multiplexes (10-20 eV windows about selected elemental lines). After removal of X-ray satellites, background subtraction, and correction for inelastic scattering, spectra were fit to Gaussian-Lorentzian line shapes to determine

center, full width at half-maximum (FWHM), and integrated area of each peak. All binding energies were referenced to adventitious carbon, C 1s = 284.80 eV; the spectrometer work function was set using the Au $4f_{7/2}$ line (84.0 eV) and the linearity of the energy scale calibrated using the Cu $2p_{3/2}$, Cu Auger, and Cu 3p lines.[19] Binding energy corrections were normally <0.2 eV because all samples were conductors and were grounded to the spectrometer either by means of the Cu wire from the back contacts of photoelectrodes or by mounting crystals with conducting graphite paint. Sputter-cleaned surfaces were obtained using a 5 keV Ar ion beam, ~100 $\mu A/cm^2$, rastered over a 3 x 3 mm area, for 5 min.

Chemicals. HPLC grade CH_3CN (Baker) was purified and dried by distillation from P_2O_5 and stored over 4 A molecular sieves. Tetrabutylammonium tetrafluoroborate was obtained from Southwestern Analytical Co. (Austin, TX) and dried at 70°C for at least 24 h. Redox reagents employed in this investigation were either obtained commercially or synthesized by standard techniques. Their preparation and/or purification have been reported elsewhere.[20] The 1,2-dicyanobenzene was recrystallized from hot toluene. All other reagents were used without purification.

Results and Discussion

Cyclic Voltammetry of Various Redox Couples at p-CdTe

The cyclic voltammetry of a number of redox species at reduced and oxidized p-CdTe was examined in order to determine the influence of surface etching procedures on the semiconductor/electrolyte interface. In particular, we have employed redox couples that show reversible, one-electron reductions at Pt in dry CH_3CN solutions containing 0.2 M [n-Bu_4N]BF_4 as supporting electrolyte. In the absence of any specific interactions between the redox species of interest and p-CdTe (such as strong adsorption), the resulting electrochemical behavior in the dark and under illumination should be dominated by the semiconductor/electrolyte energetics and not by kinetic limitations. No specific interactions between p-CdTe (reduced or oxidized) and the redox couples employed here were discerned in this investigation or in previous studies concerning n-CdTe.[1]

Cyclic voltammetry is commonly employed to measure the photovoltages developed at illuminated semiconductor electrodes immersed in electrolyte/redox couple solutions.[21,22] The potential difference between the voltammetric wave at a reversible electrode (such as Pt) and that observed at the illuminated semiconductor represents, to a close degree, the photovoltage developed under illumination. When only one-half of the redox couple is present in solution, we have found that the difference in potential of cathodic peak current observed at Pt, $E_{pc,Pt}$, and the semiconductor electrode, $E_{pc,CdTe}$, yields satisfactory E_V values consistent with the true open-circuit photovoltage measurable when both halves of the redox couple are present. Thus, photovoltages reported herein are given by equation (2). All values of $E_{pc,CdTe}$, and thus E_V, are the average

$$E_V = |E_{pc,p\text{-}CdTe} - E_{pc,Pt}| \qquad (2)$$

values for a number of measurements at different p-CdTe electrodes and the

estimated error in these values is ± 0.1 V. The light intensity employed was ~40 mW/cm^2 for illuminated p-CdTe.

Figure 1 illustrates the differences between the electrochemical behavior of p-CdTe electrodes etched in the oxidizing etchant and those etched in the reducing etchant, when immersed in an electrolyte solution containing either 2-t-butylanthraquinone (BAQ) or N,N'-dimethyl-4,4'-bipyridinium, MV^{2+}, at ~2 mM. Both electroactive species show two, well-resolved, one-electron reductions at Pt electrodes. The electrochemical response in the dark for the first and second reductions of MV^{2+} and for the first reduction of BAQ is typical of the behavior observed at "oxidized" p-CdTe electrodes for redox couples with redox potentials positive of ~-1.0 V vs. SSCE. Reversible one-electron waves for these couples are observed at potentials corresponding closely to the values at Pt. In contrast, the electrochemical behavior of these couples in the dark at "reduced" p-CdTe is remarkably different, showing negligible cathodic currents due to the reduction of the electroactive solution species. Only a small anodic current is observed at "reduced" p-CdTe for the oxidation of some residual MV^+ present in the solution. The photoresponse of "oxidized" and "reduced" p-CdTe electrodes in these solutions is also dissimilar as shown in Figure 1. Upon illumination with 632.8 nm light, only a small increase in current is observed at "oxidized" p-CdTe for those couples that showed reversible (or "ohmic") behavior in the dark ($MV^{2+/+}$, $MV^{+/0}$ and $BAQ^{0/-}$). The second reduction of BAQ at "oxidized" p-CdTe is observed upon illumination at approximately the same potential as on Pt, but the voltammetric wave at the p-CdTe is not well resolved. It is worth pointing out that the cathodic peaks for these couples at the illuminated "oxidized" electrode, $E_{pc,CdTe}$, occur at essentially the same potential as at Pt and, thus, the photovoltage, E_V, is negligible. Illumination of the "oxidized" p-CdTe appears to slightly increase the rate of charge-transfer across the

semiconductor/electrolyte junction without affecting the potential at which the peak reduction current occurs. Reductions at "reduced" p-CdTe electrodes do not occur in the dark, but can be readily effected when the electrode is irradiated. Figure 1 shows that the reductions of BAQ occur at significantly less negative potentials than at either "oxidized" p-CdTe or at Pt. The difference in $E_{pc,Pt}$ and $E_{pc,p\text{-}CdTe(reduced)}$ is 0.16 V and 0.31 V for the first and second BAQ reduction, respectively. Similarly, MV^{2+} can be effectively photoreduced at "reduced" p-CdTe, but with smaller E_V values. The first reduction occurs at essentially identical potentials to Pt (E_V = 0.01), and only a modest photovoltage is observed for the second reduction (E_V = 0.09 V). These results and those obtained in solutions containing other redox species are listed in Table I for "reduced" and "oxidized" p-CdTe electrodes.

Comparison of voltammetric results at "reduced" and "oxidized" p-CdTe for those electroactive species having redox potentials more negative than -1.5 V vs. SSCE is difficult, due to the electrochemical reduction of the "oxidized" p-CdTe surface which gives rise to large cathodic currents and irreproducible behavior. For instance, the initial cyclic voltammogram observed for "oxidized" p-CdTe in the presence of $Ru(bpy)_3^{2+}$ shows a broad cathodic wave extending from ~-1.2 to -2.0 V vs. SSCE; this same wave is observed in the absence of $Ru(bpy)_3^{2+}$ and is assigned to the reduction of a surface tellurium/tellurium oxide layer (see Surface Analysis, below). Repeated potential cycling of the "oxidized" p-CdTe electrode from -1.0 to -2.0 V vs. SSCE eventually (~10-15 scans) results in behavior resembling that observed for p-CdTe etched in the reducing etch: negligible dark current is observed in the potential region between ~-0.4 and -2.0 V vs. SSCE, and good photovoltages can be obtained for redox couples having $E_{1/2}$ more negative than ~-0.8 V vs SSCE. Small background photocurrents are observed at potentials more negative than ~-1.5 V when no redox couple is added. This

photocurrent is possibly due to the reduction of CdTe,[23] resulting in the dissolution of the semiconductor. The response of $Ru(bpy)_3^{2+}$ and 1,2-dicyanobenzene at "reduced" p-CdTe in the dark and under illumination is shown in Figure 2. The reduction of $Ru(bpy)_3^{2+}$ at Pt shows three one-electron voltammetric waves that are well-separated (by ca. 200 mV). At illuminated "reduced" p-CdTe these three waves are significantly less resolved, showing peak separations of only 70 and 150 mV. In essence, the three reversible $Ru(bpy)_3^{2+}$ reductions, which occur at differing potentials at Pt, are observed at nearly the same electrode potential at illuminated p-CdTe, yielding E_V values of 0.38, 0.45, and 0.60 V, respectively. This behavior demonstrates nicely one of our conclusions regarding "reduced" p-CdTe: the barrier height and photovoltage depend largely on the redox potential of the contacting electrolyte solution. Photoreductions of electroactive species with quite negative potentials can also be effected at p-CdTe, as demonstrated for the case of 1,2-dicyanobenzene($E_{1/2}$ = -1.62 V vs. SSCE). The E_V for this species at p-CdTe is 0.55 V by cyclic voltammetry at $S_2O_4^{2-}/OH^-$ treated electrodes. The electroactive species studied with the most negative reduction potential, anthracene ($E_{1/2}$ = -2.0 V vs. SSCE) also gave the largest photovoltage, E_V = 0.63 V, consistent with an E_{redox} dependent barrier height at the reduced surface.

Figure 3 shows the variation in photovoltage at "reduced" p-CdTe with changes in the electrochemical potential of the contacting electrolyte solution. Values of E_V for "oxidized" p-CdTe electrodes, which were not greater than 0.1 V for any redox couple examined (Table I), are not shown. Several conclusions can be drawn from mapping out the energetics of the semiconductor/ electrolyte interface as in Figure 3. First, significant photovoltages are not observed for couples having redox potentials positive of -0.4 V. Thus, we take -0.4 V vs. SSCE to be approximately equal to the flat-band potential, E_{FB}, Scheme I. This

is in good agreement with capacitance results (vide infra). The second conclusion drawn from Figure 3 is that the photovoltages, while increasing at more negative redox potentials, do not reach values expected for an ideal junction. The largest rate of increase of E_V, i.e. $\Delta E_V/\Delta E_{redox}$, is about 0.6, considerably less than the value of 1.0 predicted from equation (3). This

$$E_V = |E_{redox} - E_{FB}| \qquad (3)$$

non-ideal behavior has been observed before for other semiconductors[24] and is probably due to direct recombination of photogenerated charge carriers within the semiconductor interior or via interfacial states. Note that the correspondence between E_V and E_{redox} is not strictly linear (i.e., $\Delta E_V/\Delta E_{redox}$ is not constant over the entire range), indicating that recombination rates are potential-dependent.

Differential Capacitance of p- and n-CdTe in CH_3CN/Electrolyte Solutions

The behavior of p-CdTe presented above and that reported earlier for n-CdTe[1] indicates that the barrier height associated with the semiconductor/electrolyte junction depends on the surface pretreatment. To gain further understanding of this phenomenon we have determined the space charge capacitance, C_{SC}, of these materials as a function of electrode potential, E_f, in CH_3CN containing only 0.2 M [n-Bu_4N]BF_4.[25] The differential capacitance has been taken to be equal to C_{SC} and has been measured as described in the Experimental. Results for both "oxidized" and "reduced" p- and n-CdTe are shown in Figure 4, along with the resulting Mott-Schottky data ($1/C_{SC}^2$ vs. E_f). These figures show typical results of a number of measurements on independently prepared CdTe electrodes. The C_{SC} vs. E_f data for "reduced" n- and p-CdTe are consistent with a variation in the band bending as the electrode potential is varied resulting in a strong variation in

C_{sc}. In contrast, C_{sc} values for CdTe electrodes etched in the oxidizing etchant are virtually independent of E_f indicating that the space charge, and thus band bending, remains constant over a wide potential range.

The general shape and magnitude of the $1/C_{sc}^2$ vs. E_f plots were found to be independent of the modulation frequency between 100 and 3000 Hz. However, significant differences in C_{sc} values were observed, even at a fixed frequency, between repetitive measurements leading to scatter in the values of intercept (±0.1 V) and slope (±20%) of the Mott-Schottky plots. This somewhat erratic behavior is due to changes in the chemical composition of the surface upon cycling the electrode potential between negative and positive values. To demonstrate this more clearly, an "oxidized" n-type CdTe electrode, which yielded a potential-independent C_{sc} value (~80 nF/cm^2), was potentiostatted at -1.8 V vs. SSCE for 15 minutes in the dark. At this potential the differential capacitance immediately begins to increase and reaches a limiting value (~700 nF/cm^2) after 10 minutes, equal to within 5% of the differential capacitance of the same electrode etched in the reducing etchant. Furthermore, the Mott-Schottky plot obtained after electrochemical reduction of the surface in the dark was similar to that obtained after chemical reduction. Because of this chemical instability of the CdTe surfaces we have not attempted systematic investigation of the frequency dependence of the capacitance. The effect of the negative electrode potential on the value of C_{sc} vs. E_f, however, does accord well with the photovoltage measurements described above where electrochemical reduction of "oxidized" p-CdTe ultimately yields good photovoltages.

The capacitance of an ideal semiconductor/electrolyte junction should obey the Mott-Schottky relationship, equation (4), at potentials where a depletion

$$[C_{sc}]^{-2} = 2(-E_B - kT/e)/n\varepsilon\varepsilon_o e \qquad (4)$$

layer is formed.[25] In equation (4) n is the donor (n-type) or acceptor (p-type) density; ε is the semiconductor dielectric constant; ε_o is the permittivity constant and e is the electronic charge. The literature value[26] of 7.2 for ε was used in all calculations. In the absence of a high density of surface states or deep donor levels a plot of $1/C_{sc}^2$ vs. E_f should be linear and have an extrapolated intercept equal to $-E_{FB}$ (the correction for kT/e being 27 mV at room temperature). Our plots of $1/C_{sc}^2$ vs. E_f, Figure 4, are linear for both "reduced" n- and p-CdTe in contact with $CH_3CN/[\underline{n}\text{-}Bu_4N]BF_4$. The extrapolated intercepts (average values for a number of determinations) yield values of E_{FB} of -1.4 V and -0.4 V vs. SSCE for n- and p-type electrodes, respectively. The donor (n-type) and acceptor (p-type) densities determined from the slopes of the Mott-Schottky plots are 2×10^{17} and 2.5×10^{15} cm^{-3}, respectively. These carrier densities allow a calculation of the separation of E_f from the top of the valence band or bottom of the conduction band in the bulk of p- or n-CdTe, respectively. For p-CdTe the valence band position, E_{VB}, can thus be calculated from equations (5) and (6)[25] where N_v is the density of states and m_h^* is the

$$N_v = 2(2\pi m_h^* kT/h^2)^{3/2} \qquad (5)$$

$$\frac{n_A}{N_v} = \exp(-(E_{VB}-E_{FB})/kT) \qquad (6)$$

effective hole mass. Using $m_h^* = 0.35\ m_e$[27] (the electron rest mass) places E_{VB} at -0.2 V vs. SSCE. A similar calculation for n-CdTe places the conduction band, E_{CB}, at -1.5 V vs. SSCE.[28] The difference between E_{VB} and E_{CB}, 1.3 V, is within experimental error of the reported band gap, 1.4 V, of CdTe. The value of E_{FB} for the "reduced" n-CdTe is, within experimental error, the same value obtained using photovoltage measurements.[1]

Comparison of the $1/C_{SC}^2$ vs. E_f plots for "oxidized" and "reduced" CdTe electrodes yields quantitative information regarding the value of the potential-independent barrier height, E_B, resulting from the oxidizing etch. We can assume that when C_{SC} for "oxidized" n- or p-CdTe equals C_{SC} for "reduced" n- or p-CdTe the band bending is the same in the "oxidized" and "reduced" n- or p-CdTe. The amount of band bending E_B is obtained by measuring the potential difference between E_{FB} (the intercept of the straight line drawn through $1/C_{SC}^2$ data for the "reduced" surface) and the potential at which the $1/C_{SC}^2$ values for both "oxidized" and "reduced" electrodes are equal. At this potential the band bending in both electrodes is the same and, since E_{FB} is fixed for the "reduced" sample, the band bending is thus measurable. From Figure 4 we observe that the difference between these two values for p-CdTe is equal to ~50 mV. Other determinations of E_B by this method for p-CdTe were in the range 5-80 mV, indicating that the band bending at "oxidized" p-CdTe is very small. This is in good agreement with the cyclic voltammetry results for "oxidized" p-CdTe which show "ohmic" behavior in the dark and photovoltages less than 100 mV for a number of electroactive species, Table I. Taking E_{FB}-E_{VB} to be ~0.2 V, from equations (5) and (6), this means that the value of E_B for "oxidized" p-CdTe is ~0.3 V. The band bending of "oxidized" n-CdTe samples, measured by the same procedure, is 0.5 - 0.7 V, a much larger value than with p-CdTe, in agreement with the observed photovoltage at such electrodes.[1,2] Thus, for "oxidized" n-CdTe the value of E_B is ~0.8 V.

The E_{redox}-independent barrier height of "oxidized" n- and p-CdTe indicates that the photovoltages developed at these electrodes are limited by Fermi level pinning and not by carrier inversion. This is unequivocal for p-CdTe where the small barrier height ($E_B \cong 0.3$ V) cannot be due to carrier inversion of a 1.4 eV band gap semiconductor.[25] The constant C_{SC} value observed for n-CdTe, even at

potentials extending 0.6 V negative of the conduction band edge (E_{CB} as measured from the Mott-Schottky plots of the "reduced" electrodes) also indicates that the band bending is limited by Fermi level pinning. Even if carrier inversion were important for "oxidized" n-CdTe it is necessary to conclude from Figure 4 that surface levels initially pin the Fermi level to a potential positive enough to create an accumulation of minority carriers at potentials negative of E_{CB}.

In related investigations,[29] the differential capacitance curves of p-Si in the presence of a number of redox couples show that Fermi level pinning controls the extent of band bending in that material. These results, however, are considerably different from the results reported here. The shape of the C_{SC} vs. E_f curves for p-Si is found to be independent of the contacting solution and closely resembles expectations for an ideal extrinsic p-type semiconductor (similar in shape to the capacitance-potential curve for "reduced" p-CdTe, Figure 4). However, it is found that the differential capacitance curves are shifted along the potential axis depending on the redox potential of the solution electroactive species. A linear relationship between E_{FB}, determined from the Mott-Schottky plots, and E_{redox} is observed over a considerable potential range. The p-Si in solvent/electrolyte solution containing no redox couple also gives a nearly ideal Mott-Schottky plot. The point is we conclude that "oxidized" CdTe is Fermi level pinned and yet the value of C_{SC} is invariant with changes in E_f. Changes in E_f for "oxidized" CdTe apparently give changes in the Helmholtz capacitance, not in C_{SC}. The difference in behavior of CdTe and p-Si can be understood by noting that accumulation of surface charge can occur by either of two mechanisms: (1) equilibration of the semiconductor bulk with its surface, i.e., electrons are driven to surface states of a p-type semiconductor creating a net negative surface charge or (2) equilibration of solution redox reagents with the semiconductor surface, i.e. electron-transfer from a solution donor species

to the surface states. The latter mechanism is apparently responsible for the behavior of p-Si and is consistent with a non-uniform and low density of surface states that are not able to exchange electrons with bulk p-Si. For CdTe there appears to be essentially a continuum of states between E_{VB} and E_{CB}, because the overlayer for the "oxidized" CdTe is Te° (vide infra), a small gap semiconductor. We attempted to measure C_{sc} in the presence of various redox couples, but leakage currents precluded meaningful results.

X-Ray Photoelectron Spectroscopy of CdTe Surfaces

X-ray photoelectron spectroscopy of CdTe surfaces reveals substantial differences in surface composition and chemistry of samples treated with the oxidizing vs. the reducing etch. Precise core electron binding energies were measured for the Cd $3d_{5/2,3/2}$, Te $3d_{5/2,3/2}$, and C 1s levels of each sample. A low resolution survey scan was also taken to reveal impurities and to quantitate any oxide present. Table II summarizes XPS data obtained from the various samples; values given are the average of 4 to 6 runs. The similarity of the Cd 3d binding energies of oxidized, reduced, and sputtered samples indicates there is no major variation in the chemical state of Cd. In particular, none of the Cd 3d binding energies is characteristic of Cd° or CdO, ruling out these species as major surface constituents.[30] Substantial variation is found, however, in the Te 3d region, as illustrated in Figure 5 and indicated in Table II. In addition to altering the Te chemical state, the type of etch also affects surface stoichiometry, as summarized in Table II.

The Te 3d XPS data for CdTe treated with the oxidizing etch (Figure 5, top) reveals two sets of Te $3d_{5/2,3/2}$ bands split by ~3.2 eV. The higher binding energy set, several eV higher than either Te^{2-} or Te° (as measured for sputtered CdTe and Te°, respectively) is assigned to TeO_2, the lowest stable oxide of Te,[31] in agreement with assignments made elsewhere for the Te 3d levels of air-cleaved

CdTe[32] and in agreement with the $3d_{5/2}$ binding energy reported for TeO_2 (575.9 eV).[33] The lower binding energy set of bands, lying midway between Te° and Te^{2-}, results from both Te° and underlying (bulk) CdTe; deconvolution of this rather broad (FWHM ~1.8 eV) set of bands yields two sets of bands separated by ~1 eV, the difference between Te° and Te^{2-} (Table II). Angularly resolved XPS data obtained by others[32] indicate that Te° and TeO_2 are present over similar electron escape depths. The layer of Te°/TeO_2 found on CdTe treated with the oxidizing etch is not thick, as indicated by the presence and intensity of the Cd^{2+} and Te^{2-} 3d signals and the Te/Cd ratio of 1.6 (Table II). This contrasts the results of others, including researchers in this laboratory, who have found the same or similar oxidizing etches to give Te° and/or TeO_2 films thick enough to obscure the Cd signal.[1,34,35] This discrepancy is attributable to a short delay between etching and rinsing the samples.[36] Auger depth profile data indicate that the O signal falls off rapidly as the CdTe bulk is approached, suggesting a Te°-rich layer in contact with bulk CdTe.[36]

The Te 3d spectrum for CdTe treated with the reducing etch, Figure 5, second from top, closely resembles that of sputter cleaned CdTe, third from top, implying that the reducing etch leaves a surface which resembles pure CdTe chemically; the difference in Te $3d_{5/2}$ binding energies is only 0.03 eV (Table II). The sputtered and reduced CdTe surfaces resemble one another stoichiometrically as well, both having a Cd/Te ratio of one (Table III). In addition to the predominant Te^{2-} peak, the reduced surface spectrum has a small, high energy band attributable to TeO_2 from air oxidation of the surface;[37] the spectra of some reduced CdTe samples showed asymmetry on the high energy side of the Te^{2-} peak, suggesting the presence of a small amount of Te°.

Sputter-cleaned CdTe and Te° have X-ray photoelectron spectra containing only a single set of Te 3d bands (Figure 5), giving the 3d binding energies of

Te^{2-} and Te°, respectively (Table II). The spectrum of unsputtered (air oxidized) elemental Te (Figure 5, second from bottom) shows a small peak due to Te° and a much larger peak attributable to TeO_2,[33] indicating that Te° films formed on CdTe by an oxidizing etch are likely to be partially air-oxidized to TeO_2. In fact, allowing "reduced" CdTe samples to stand in air for ~2 weeks caused the small band attributed to TeO_2 to grow in intensity, indicating the Te^{2-} on the surface of CdTe is slowly air oxidized to TeO_2.[37]

The XPS studies indicate that the "oxidized" CdTe can be viewed as a situation where the bulk CdTe is coated with Te°.[1,36] Thus, the space charge layer in the CdTe arises from the equilibration of CdTe with Te° just as for deliberately prepared heterojunctions such as CdTe/metal Schottky barriers. Interestingly, Te° is a large work function material[38] and would be expected, therefore, to give a larger barrier height on n-CdTe than on p-CdTe. We find that the sum of the barrier heights for "oxidized" n- and p-CdTe is ~1.1 V, somewhat less than the 1.4 eV band gap would predict. However, the error in the values of E_B are at least ±0.1 V. Scheme II summarizes our view of the interface for "oxidized" CdTe where the space charge layer in the CdTe region is controlled by the Te°/TeO_2 overlayer. The "reduced" CdTe behaves as a nearly ideal semiconductor[3,4] when in contact with electrolyte solutions. However, the photovoltage vs. E_{redox}, Figure 3, suggests recombination losses at the positive E_{redox} values, since there is significant curvature several tenths of a volt more negative than E_{FB}.

Photoelectrochemical Energy Conversion Using p-CdTe-Based Cells

The improvement in the ideality of n-CdTe using a reductive surface pretreatment cannot be easily exploited to improve the energy conversion efficiency for n-CdTe photoanode-based electrochemical cells. This is because

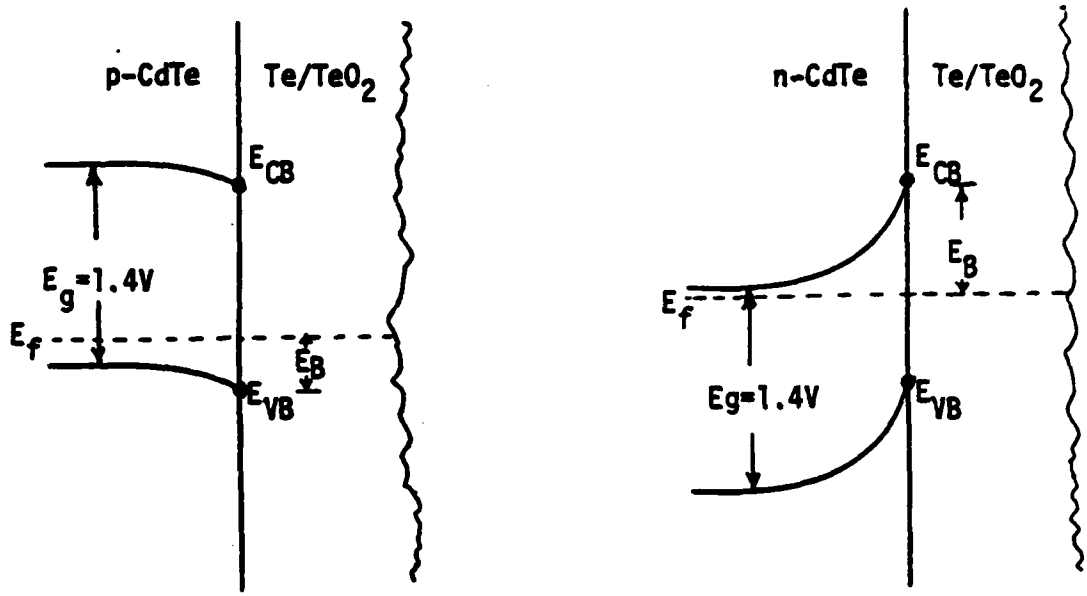

Scheme II. Representation of the CdTe/Te/TeO_2 interfaces resulting from an oxidative pretreatment of p-CdTe (left) and n-CdTe (right) showing a larger barrier height, E_B=0.8V ±0.1V, on n-CdTe than on p-CdTe, E_B=0.3V ± 0.1V.

the photoanodic decomposition of the surface of n-CdTe leads to rapid degradation of the improved barrier height, even though gross photocorrosion could likely be suppressed.[1] However, the improvement of p-CdTe could possibly be exploited, provided very negative redox couples are employed, Figure 3. Indeed, the capacitance measurements of "oxidized" p-CdTe held at a negative potential indicate that nearly ideal behavior can be induced by electrochemical reduction. Thus, p-CdTe could be protected from degradation under illumination when electrons are driven to the surface. Accordingly, we have demonstrated that a p-CdTe-based photoelectrochemical cell can be efficient when using a sufficiently negative redox couple.

Figure 6 shows the steady-state photocurrent-voltage curves observed at "reduced" p-CdTe immersed in a 0.1 M 1,2-dicyanobenzene/CH_3CN/[n-Bu_4N]BF_4 solution. As expected from the cyclic voltammetric response, Figure 2, cathodic photocurrents are observed only when the electrode is irradiated. The onset of photocurrent begins at ~-0.8 V vs. SSCE which is ~0.7 V more positive than the onset of current at Pt. In essence, the reduction of 1,2-dicyanobenzene is driven at a light intensity limited rate at illuminated p-CdTe with a potential savings of ~0.7 V relative to its thermodynamic reduction potential. The quantum yield, fill factor, and power conversion efficiency at various light intensities are listed in Table III for three different photoelectrochemical cells, including one where the solution potential was poised by having a significant concentration of both halves of the redox couple. Interestingly, the photovoltage observed is up to 0.9 V, rivalling the best semiconductor photocathodes reported.[22] We note that the quantum yield for electron flow at short-circuit, Φ_e, is uncorrected for losses due to surface reflection which may be substantial on the shiny p-CdTe surfaces. However, Φ_e is large, ~0.6, and shows only a small decrease with increasing light intensity indicating that the photoresponse is not dominated by

large recombination rates of electron-hole pairs at short-circuit. The wavelength dependence of Φ_e shows an onset of photoresponse at E_g with a sharp rise at slightly higher energy, consistent with the fact that CdTe is a direct band gap semiconductor.[13] The fill factor, which is a measure of the rectangularity of the photocurrent-voltage curves, is given by equation (7) where

$$\text{Fill Factor} = \frac{(i \times E_V)_{max}}{E_V(oc) \times i_{sc}} \tag{7}$$

$(i \times E_V)_{max}$ is the maximum power delivered by the photoelectrochemical cell. Values of the fill factor were in the range 0.4-0.5, decreasing with increasing light intensity. The maximum power conversion efficiency, η_{max}, given by equation (8) is ~8-10% for the reduction of the [1,2-dicyanobenzene]$^{0/-}$ system

$$\eta_{max} = \frac{(i \times E_V)_{max}}{\text{input power}} \times 100 \tag{8}$$

using 632.8 nm input optical energy.

The overall chemistry of this photoelectrochemical cell is given by:

$$[1,2\text{-dicyanobenzene}]^0 + e^- \rightarrow [1,2\text{-dicyanobenzene}]^- \text{ (p-CdTe photocathode)}$$

$$[1,2\text{-dicyanobenzene}]^- \rightarrow [1,2\text{-dicyanobenzene}]^0 + e^- \text{ (Pt counterelectrode)}$$

The [1,2-dicyanobenzene]$^-$ photogenerated at p-CdTe is oxidized at the counterelectrode resulting in no net chemical change. The short-circuit current response under ~30 mW/cm^2 of 632.8 nm light slowly declines after about 1 h of operation. Although we have not investigated this instability in detail, loss of [1,2-dicyanobenzene]$^-$ occurs due to irreversible reactions with trace H_2O present in solution. The need to use very negative redox couples will likely be an impediment to practical photoelectrochemical energy conversion devices based on p-CdTe.

Conclusions

The photoelectrochemical behavior of p-CdTe immersed in electrolyte solutions has been shown to be strongly dependent on the nature of the surface pretreatment. As previously shown with n-CdTe photoanodes,[1] etching the photoelectrode with an oxidizing etch results in a constant photovoltage upon illumination independent of the solution redox potential. This behavior has now been shown by XPS to result from a thin TeO_2/Te° surface layer which introduces a high density of surface levels capable of accumulating enough charge to shift the band edge positions with variation in E_{redox}. This situation is referred to as Fermi level pinning and dominates the behavior of p- or n-type CdTe etched by $Cr_2O_7^{2-}/HNO_3$ solutions. In contrast, p- and n-CdTe electrodes[1] etched by $S_2O_4^{2-}/OH^-$ behave in a more ideal fashion showing photovoltages that vary considerably with E_{redox}. Surface analysis reveals that the surface of such electrodes closely resembles bulk CdTe.

An important conclusion from these studies is that barrier height of "oxidized" p- or n-type CdTe, as measured by the differential capacitance, agrees quite well with the value inferred from photovoltage determinations, i.e. $E_B \equiv E_V(max)$. This relationship is often assumed in photoelectrochemical studies[1,2,4,5] and the results presented here demonstrate its validity, at least in the case of CdTe photoelectrodes. Conventional electrochemical techniques, e.g. cyclic voltammetry, thus appear to be reliable means of mapping out the energetics of the semiconductor/electrolyte interface.

Modification of the p-CdTe surface by etching in $S_2O_4^{2-}/OH^-$ solutions has been demonstrated to yield relatively efficient photocathodes for the reduction of 1,2-dicyanobenzene. The visible light power conversion efficiency is considerably larger than previously reported[11] values for p-CdTe-based photoelectrochemical cells and represents the first efficient photoelectrochemical cell

based on a p-type II-VI compound. We are presently extending these investigations to another II-VI semiconductor, p-ZnTe, which will be the subject of a future report. Finally, we note that work on CdTe/metal Schottky barriers has generally employed an oxidative pretreatment of the CdTe.[15,39] Our results indicate that different results could obtain for a reductive pretreatment.

Acknowledgements. This work was supported in part by the Office of Naval Research. Use of the Central Facilities of the M.I.T. Center for Materials Science and Engineering is gratefully acknowledged. A.J.R. acknowledges support as a NPW Predoctoral Fellow at M.I.T., 1982-1983.

References

1. Tanaka, S.; Bruce, J.A.; Wrighton, M.S. J. Phys. Chem., 1981, 85, 3778.
2. Aruchamy, A.; Wrighton, M.S. J. Phys. Chem., 1980, 84, 2848.
3. Gerischer, H. in "Physical Chemistry: An Advanced Treatise", Eyring, H.; Henderson, D.; Jost, W., eds., Vol. 9A, Academic Press:New York, 1970.
4. Gerischer, H. J. Electroanal. Chem., 1975, 58, 263.
5. Frank, S.N.; Bard, A.J. J. Am. Chem. Soc., 1975, 97, 7427.
6. Bard, A.J.; Bocarsly, A.B.; Fan, F.-R.F.; Walton, E.G.; Wrighton, M.S. J. Am. Chem. Soc., 1980, 102, 3671.
7. Ellis, A.B.; Kaiser, S.W.; Wrighton, M.S. J. Am. Chem. Soc., 1976, 98, 1635.
8. Ellis, A.B.; Bolts, J.M.; Wrighton, M.S. ibid., 1977, 99.
9. Hodes, G.; Manassen, J.; Cahen, D. J. Appl. Electrochem., 1977, 7, 181.
10. Miller, B.; Heller, A. Nature (London), 1976, 262, 680.
11. (a) Bockris, J. O'M.; Uosaki, K. J. Electrochem. Soc., 1977, 124, 1348; (b) Nadjo, L. J. Electroanal. Chem., 1980, 108, 29; (c) Bolts, J.M.; Ellis, A.B.; Legg, K.D.; Wrighton, M.S. J. Am. Chem. Soc., 1977, 99, 4826.
12. Crowder, B.L.; Hammer, W.N. Phys. Rev., 1966, 150, 541.
13. Strauss, A.J. Rev. Phys. Appl., 1977, 12, 167.
14. "American Physical Society Study Group on Photovoltaic Energy Conversion", H. Ehrenreich, Chairman, The American Physical Society:New York, 1979.
15. Ponpon, J.P.; Saraphy, M.; Buttung, E.; Siffert, P. Phys. Status Solidi, 1980, 57, 259.
16. Aven, M.; Garwacki, W. J. Electrochem. Soc., 1967, 114, 1063.
17. Bard, A.J.; Faulkner, L.R. in "Electrochemical Methods, Fundamentals and Applications", J. Wiley & Sons:New York, 1980.

18. The software for computer control of the XPS spectrometer, as well as data acquisition and curve fitting, is part of the MACS (Version VI) software package: Physical Electronics Division, Perkin-Elmer Corp., Eden Prairie, MN.

19. Wagner, C.D. "Energy Calibration of Electron Spectrometers", Applied Surface Analysis, ASTM STP 699, Barr, T.L.; Davis, L.E., eds., American Society for Testing and Materials, 1980, pp. 137-147.

20. (a) Schneemeyer, L.F.; Wrighton, M.S. J. Am. Chem. Soc., 1980, 102, 6964; (b) ibid., 1979, 101, 6496; (c) Bocarsly, A.B.; Bookbinder, D.C.; Dominey, R.N.; Lewis, N.S.; Wrighton, M.S. ibid., 1980, 102, 3683.

21. Kautek, W.; Gerischer, H. Ber. Bunsenges. Phys. Chem., 1980, 84, 645; White, H.S.; Fan, F.-R.F.; Bard, A.J. J. Electrochem. Soc., 1981, 128, 1045; Kohl, P.A.; Bard, A.J. J. Am. Chem. Soc., 1977, 99, 7531.

22. Baglio, J.A.; Calabrese, G.S.; Harrison, D.J.; Kamieniecki, E.; Ricco, A.J.; Wrighton, M.S.; Zoski, G.D. J. Am. Chem. Soc., 1983, 105, 2246 and references therein.

23. Bard, A.J.; Wrighton, M.S. J. Electrochem. Soc., 1977, 124, 1706.

24. Fan, F.-R.F.; White, H.S.; Wheeler, B.; Bard, A.J. J. Am. Chem. Soc., 1980, 102, 5142.

25. For a detailed description of the semiconductor/electrolyte junction capacitance, see Myamlin, V.A.; Pleskov, Y.V. in "Electrochemistry of Semiconductors", Plenum Press:New York, 1967.

26. van Vechten, J.A. Phys. Rev., 1969, 182, 899.

27. Values of 0.35 and 0.14 for the effective hole and electron mass of CdTe, respectively, were taken from the "Handbook of Chemistry and Physics", Vol. 51, Robert C. Weast, Ed., The Chemical Rubber Co., Cleveland, OH, 1970-1971. Slightly different values, 0.8 (m_h^*) and 0.10 (m_e^*) are given in ref. 13.

These differences do not appreciably change the values of E_{CB} or E_{VB} calculated using equations (5) and (6).

28. In calculating the position of the conduction band edge, E_{CB}, m_e^* is substituted for m_h^* in equation (5) and (E_{FB} - E_{CB}) is substituted for (E_{VB} - E_{FB}) in equation (6).

29. (a) Nagasubramanian, G.; Wheeler, B.L.; Fan, F.-R.F.; Bard, A.J. J. Electrochem. Soc., 1982, 129, 1743; (b) Kerita, B.; Kawenoki, I.; Kossanyi, J.; Garreau, D.; Nadjo, L. J. Electroanal. Chem., 1983, 145, 293.

30. Gaarenstroom, S.W.; Winograd, N. J. Chem. Phys., 1977, 67, 3500.

31. Cotton, F.A.; Wilkinson, G. "Advanced Inorganic Chemistry", 4th ed., John Wiley & Sons:New York, 1980, p. 527.

32. Patterson, M.H.; Williams, R.H. J. Phys. D.: Appl. Phys., 1978, 11, L83.

33. Bahl, M.K.; Watson, R.L.; Irgolic, K.J. J. Chem. Phys., 1977, 66, 5526.

34. (a) Zitter, R.N.; Charda, D.L. J. Appl. Phys., 1975, 46, 1405; (b) Zitter, R.N. Surf. Sci., 1971, 28, 335.

35. Gaugash, P.; Milnes, A.G. J. Electrochem. Soc., 1981, 128, 924.

36. Ricco, A.J.; White, H.S.; Wrighton, M.S. J. Vac. Sci. Technol., submitted.

37. Hage-Ali, M.; Stuck, R.; Saxena, A.N.; Siffert, P. Appl. Phys., 1979, 19, 25.

38. Sze, S.M. "Physics of Semiconductor Devices", 2nd ed., John Wiley & Sons: New York, 1981, p. 251.

39. (a) Ponpon, J.P. Appl. Phys. A, 1982, 27- 11 and references therein; (b) Anthony, T.C.; Fahrenbruch, A.L.; Bube, R.H. J. Electron. Mtls., 1982, 11, 89.

Table I. Results from Cyclic Voltammetry of Various Redox Couples at Reduced and Oxidized p-CdTe.

Redox Couple, no.[a]	$E_{1/2}$[b,c]	Reduced p-CdTe				Oxidized p-CdTe		
		$E_{pc,Pt}$	$E_{pc,CdTe}$	E_y,V[d]	Dark Behavior[e]	$E_{pc,CdTe}$	E_y,V[d]	Dark Behavior[e]
$TCNQ^{0/-}$, 1	0.15	0.20	-----	-----	ohmic	0.11	0	ohmic
$TCNQ^{-/2-}$, 2	-0.35	-0.40	-0.52	0	rectifying	-0.46	0	ohmic
$MV^{2+/+}$, 3	-0.43	-0.47	-0.46	0.01	rectifying	-0.47	0	ohmic
$MV^{+/0}$, 4	-0.84	-0.89	-0.80	0.09	rectifying	-0.88	0.01	ohmic
$BAQ^{0/-}$, 5	-0.93	-0.97	-0.81	0.16	rectifying	-1.01	0	ohmic
$Ru(bpy)_3^{2+/+}$, 6	-1.32	-1.36	-0.98	0.38	rectifying	-1.30	0.06	ohmic
$BAQ^{-/2-}$, 7	-1.51	-1.60	-1.20	0.40	rectifying	----[f]	---[f]	rectifying
$Ru(bpy)_3^{+/0}$, 8	-1.52	-1.55	-1.11	0.45	rectifying	-1.64	0	ohmic
1,2-$DCB^{0/-}$, 9	-1.62	1.68	-1.13	0.55	rectifying	-----	-----	-----
$Ru(bpy)_3^{0/-}$, 10	-1.77	-1.81	-1.21	0.60	rectifying	-1.82	0	ohmic
$An^{0/-}$, 11	-2.01	-2.06	-1.43	0.63	rectifying	-----	-----	-----

[a]All data are for CH_3CN/0.2 M $[n\text{-}Bu_4N]BF_4$ solutions at 25°C. Scan rates are 5-100 mV/sec. Redox reagent concentrations are 1-3 mM. TCNQ is tetracyanoquinodimethane; MV is N,N'-dimethyl-4,4'-bipyridinium; BAQ is 2-t-butyl-9,10-anthraquinone; bpy is 2,2'-bipyridine; DCB is dicyanobenzene; and An is anthracene. The numbers after each redox couple refer to the data points in Figure 3.

[b]All potentials referenced to SSCE.

[c]$E_{1/2}$'s calculated from cyclic voltammetry data according to $E_{1/2} = (E_{pa} + E_{pc})/2$ where E_{pa} and E_{pc} refer to potentials of the anodic and cathodic peak current.

[d]Cf. equation (2) of text. Illumination provided by a He-Ne laser (632.8 nm) at ~40 mW/cm^2.

[e]"Ohmic" and "rectifying" refer to the presence and absence, respectively, of a well-defined cyclic voltammetric wave in the dark due to the reduction of the electroactive species.

[f]No well-defined peak-potential was observed for $BAQ^{-/2-}$ at illuminated p-CdTe (see Figure 1 and text).

Table II. Summary of XPS Data for Chemical State and Stoihciometry of Oxidized, Reduced, and Ion-Sputtered CdTe[a]

Surface Examined	Signals Observed, eV	Relative Intensity [b]	Assignment, Core Level	
Sputtered CdTe	405.08(6)	1.0	Cd^{2+}	$3d_{5/2}$
	411.84(6)			$3d_{3/2}$
	572.47(5)	1.1(1)	Te^{2-}	$3d_{5/2}$
	582.87(4)			$3d_{3/2}$
"Reduced" CdTe	404.94(7)	1.0	Cd^{2+}	$3d_{5/2}$
	411.69(6)			$3d_{3/2}$
	572.50(7)	1.0(3)	Te^{2-}	$3d_{5/2}$
	582.92(7)			$3d_{3/2}$
	575.96(11)	0.04(5)	TeO_2	$3d_{5/2}$
	586.27(15)			$3d_{3/2}$
"Oxidized" CdTe	405.15(7)	1.0	Cd^{2+}	$3d_{5/2}$
	411.90(8)			$3d_{3/2}$
	572.98(11)	1.2(1)	"Mixed"	$3d_{5/2}$
	583.40(11)		Te^{2-}/Te°	$3d_{3/2}$
	576.21(10)	0.4(2)	TeO_2	$3d_{5/2}$
	586.58(10)			$3d_{3/2}$
Air oxidized Te	573.5	0.05	Te°	$3d_{5/2}$
	583.8			$3d_{3/2}$
	576.4	1.0	TeO_2	$3d_{5/2}$
	586.8			$3d_{3/2}$
Sputtered Te	573.54	1.0	Te°	$3d_{5/2}$
	583.92			$3d_{3/2}$

[a]Each tabulated value is the average of 4-6 runs. Uncertainty in the last digit of each entry, given parenthetically, is estimated as twice the uncertainty of the average. More extensive data is published elsewhere.[36]

[b]Relative intensities are calculated from integrated peak areas of the curve fit data and are corrected for atomic sensitivity factors: Wagner, C.D.; Davis, L.E.; Zeller, M.V.; Taylor, J.A.; Raymond, R.H.; Gale, L.H. Surf. Interface Anal., 1981, 3, 211.

Table III. Efficiency for Photoreduction of 1,2-Dicyanobenzene at Illuminated p-CdTe in CH_3CN/0.2 M [n-Bu_4N]BF_4.

Electrode[a]	Solution[b]	Input Pwr[c]	$E_V(oc)$, V[d]	Φ_e[e]	f.f.[f]	η[g]
1	0.1 M 1,2-DCB	22 mW/cm^2	0.70	0.51	0.43	7.9
	(unpoised)	11.6	0.70	0.56	0.44	8.6
		6.5	0.70	0.54	0.45	8.5
2	0.1 M 1,2-DCB	40.0	0.75	0.49	0.46	8.7
	(unpoised)	20.0	0.74	0.51	0.50	9.5
		10.3	0.72	0.55	0.52	10.5
		5.2	0.70	0.54	0.54	10.4
3	0.1 M 1,2-DCB/	38.7	0.92	0.48	0.28	6.2
	2 mM 1,2-DCB$^-$	21.9	0.92	0.52	0.36	8.7
	(poised; E_{redox} =	6.1	0.90	0.51	0.44	10.3
	-1.50 V vs. SSCE)	3.0	0.82	0.55	0.48	10.9

[a]1,2 and 3 refer to different electrodes.

[b]Stirred and purged with Ar.

[c]Input irradiation at 632.8 nm.

[d]$E_V(oc)$ is the open-circuit photovoltage.

[e]Quantum yield for electron flow at E_{redox}. Data are uncorrected for reflection losses or losses from redox couple absorption.

[f]Defined by equation (7) in text.

[g]Defined by equation (8) in text.

Figure Captions

Figure 1. Comparison of cyclic voltammetry of 2-t-butylanthraquinone, 2-t-BAQ, and N,N'-dimethyl-4,4'-bipyridinium, MV^{2+}, at Pt with surface "oxidized" and "reduced" p-CdTe (illuminated, ——; dark, ----). Irradiation was at 632.8 nm, ~40 mW/cm^2.

Figure 2. Comparison of cyclic voltammetry of $Ru(bpy)_3^{2+}$ and 1,2-dicyanobenzene at Pt with surface "reduced" p-CdTe (illuminated, ——; dark, ----). Irradiation was at 632.8 nm, ~40 mW/cm^2.

Figure 3. Plot of photovoltage at "reduced" p-CdTe as a function of $E_{1/2}$ for various redox couples. Redox couples are identified by number listed in Table I. Photovoltage is as defined in text, equation (2).

Figure 4. Comparison of differential capacitance and the resulting Mott-Schottky plots for surface oxidized (----) and reduced (——) p- and n-type CdTe at a modulation frequency of 1000 Hz.

Figure 5. X-ray photoelectron spectra of the Te 3d region showing, from top: $HNO_3/Cr_2O_7^{2-}$-oxidized CdTe; $S_2O_4^{2-}/OH^-$-reduced CdTe; Ar ion sputtered CdTe; air oxidized elemental Te; and Ar ion sputtered elemental Te.

Figure 6. Steady-state photocurrent-potential curves for p-CdTe in CH_3CN/0.2 M $[n\text{-}Bu_4N]BF_4$ containing 0.1 M 1,2-dicyanobenzene. Electrodes were illuminated at 632.8 nm with a He-Ne laser at an input irradiation power as noted.

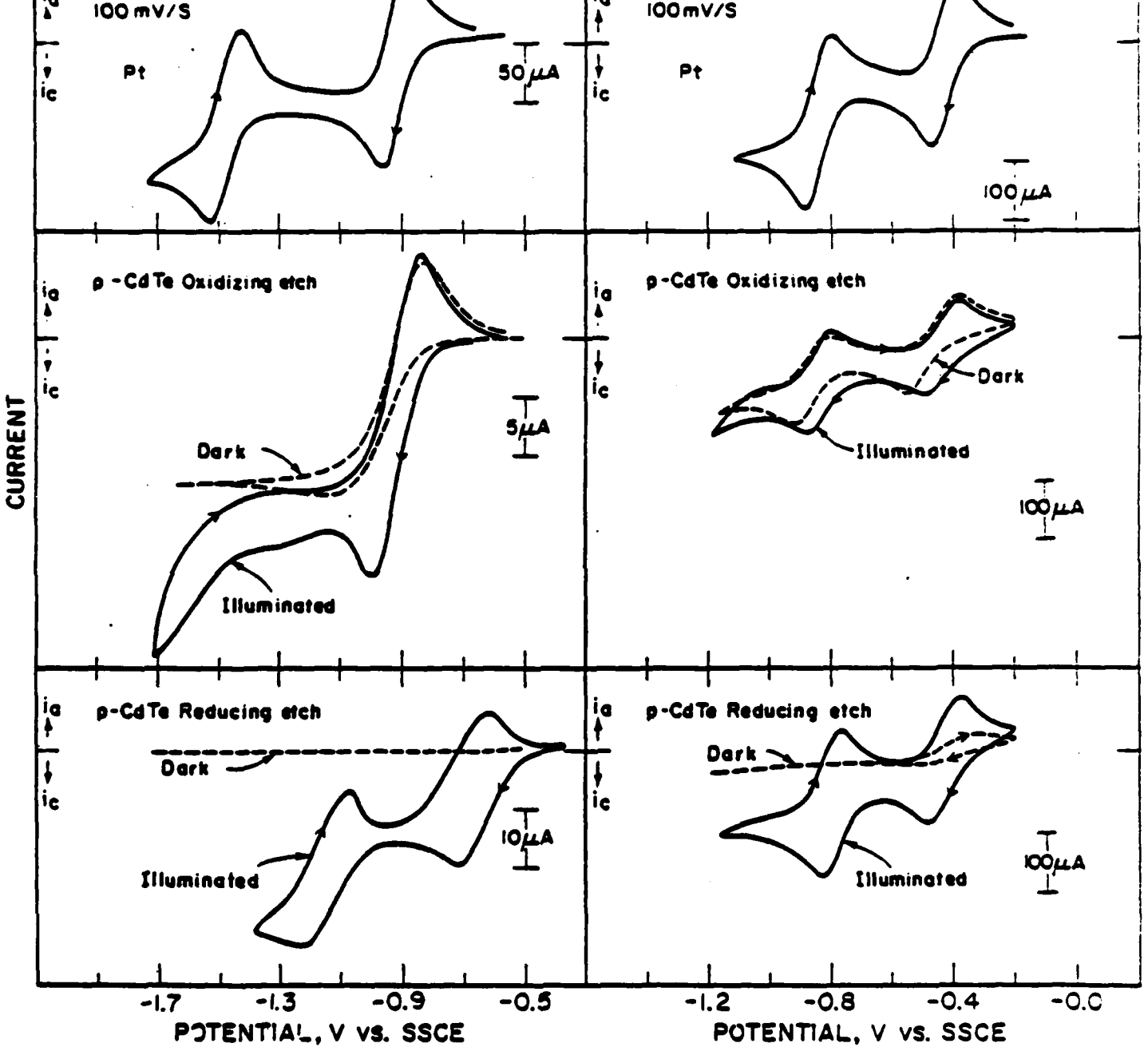
2-t-BAQ
CH3CN/0.2M[n-Bu4N]BF4
100 mV/S
Pt
50 μA
MV2+
CH3CN/0.2M[n-Bu4N]BF4
100 mV/S
Pt
100 μA
p-CdTe Oxidizing etch
Dark
Illuminated
5 μA
p-CdTe Oxidizing etch
Dark
Illuminated
100 μA
p-CdTe Reducing etch
Dark
Illuminated
10 μA
p-CdTe Reducing etch
Dark
Illuminated
100 μA
ia
ic
CURRENT
-1.7
-1.3
-0.9
-0.5
POTENTIAL, V vs. SSCE
-1.2
-0.8
-0.4
-0.0
POTENTIAL, V vs. SSCE

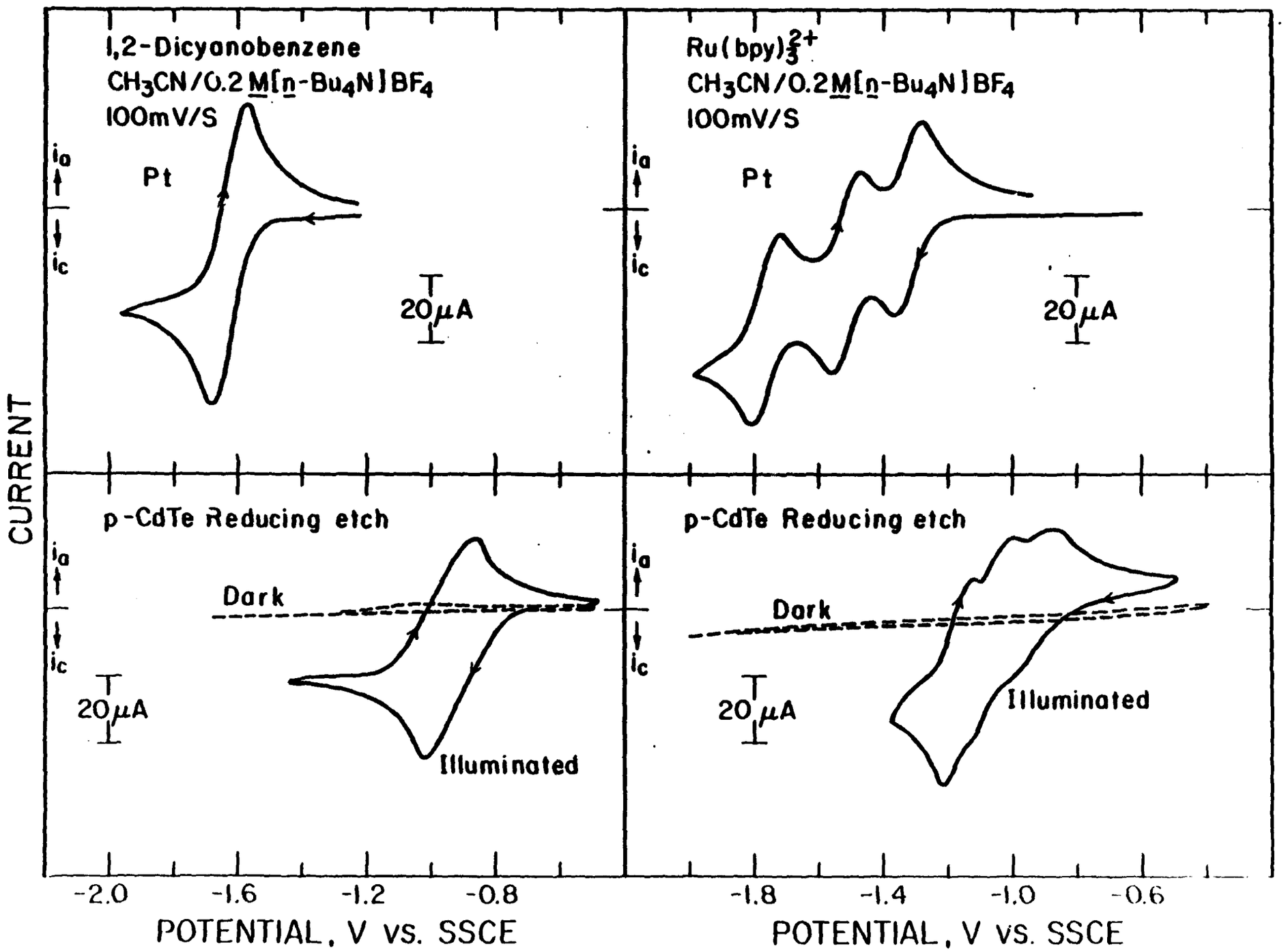
1,2-Dicyanobenzene
CH3CN/0.2 M[n-Bu4N]BF4
100mV/S
Pt
ia
ic
20μA
Ru(bpy)3 2+
CH3CN/0.2 M[n-Bu4N]BF4
100mV/S
Pt
ia
ic
20μA
p-CdTe Reducing etch
Dark
Illuminated
ia
ic
20μA
p-CdTe Reducing etch
Dark
Illuminated
ia
ic
20μA
CURRENT
-2.0
-1.6
-1.2
-0.8
POTENTIAL, V vs. SSCE
-1.8
-1.4
-1.0
-0.6
POTENTIAL, V vs. SSCE

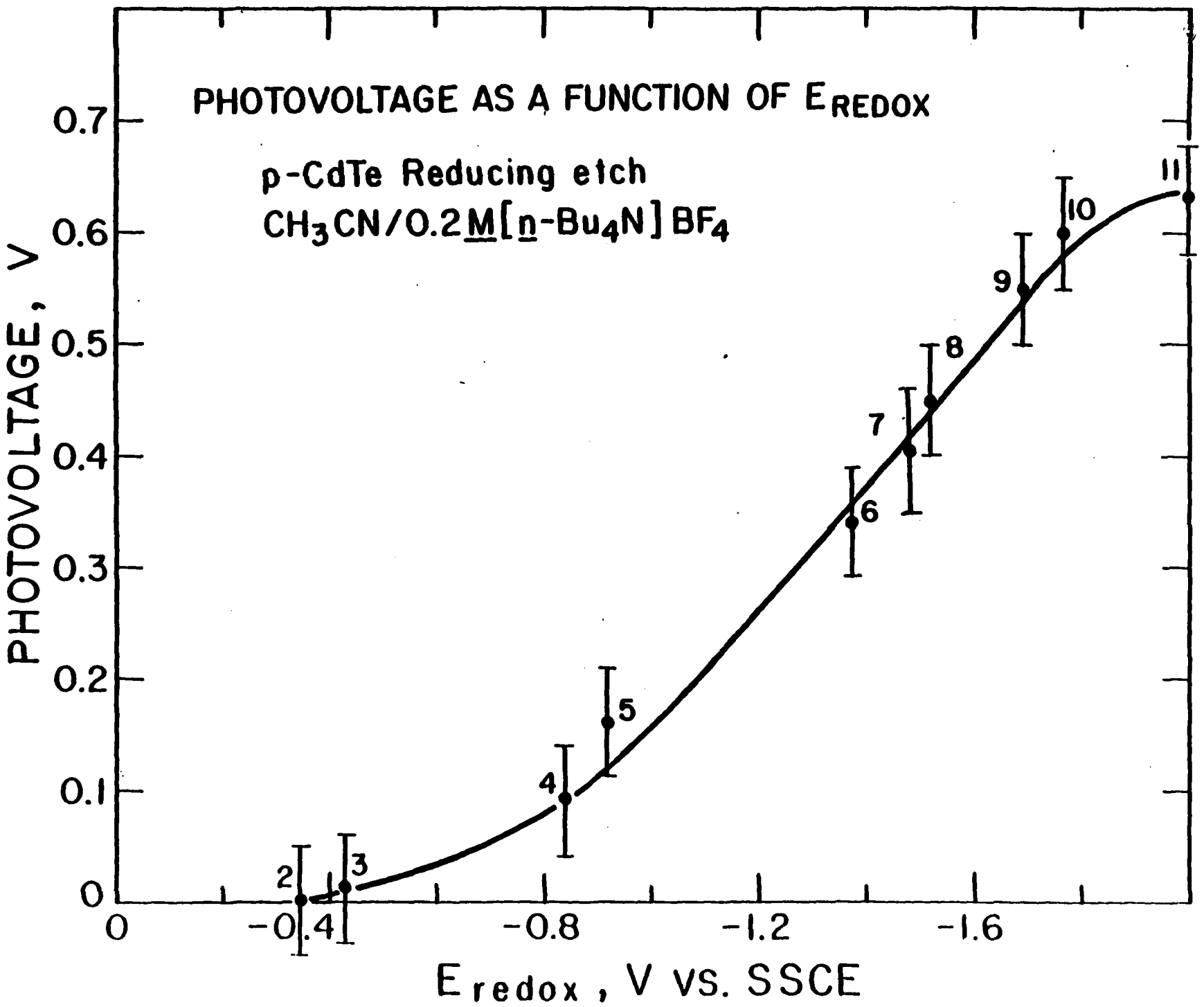
PHOTOVOLTAGE AS A FUNCTION OF E_{REDOX}
p-CdTe Reducing etch
$CH_3CN/0.2\underline{M}[\underline{n}\text{-}Bu_4N]BF_4$
PHOTOVOLTAGE, V
0.7
0.6
0.5
0.4
0.3
0.2
0.1
0
0
-0.4
-0.8
-1.2
-1.6
E_{redox}, V vs. SSCE
1
2
3
4
5
6
7
8
9
10
11

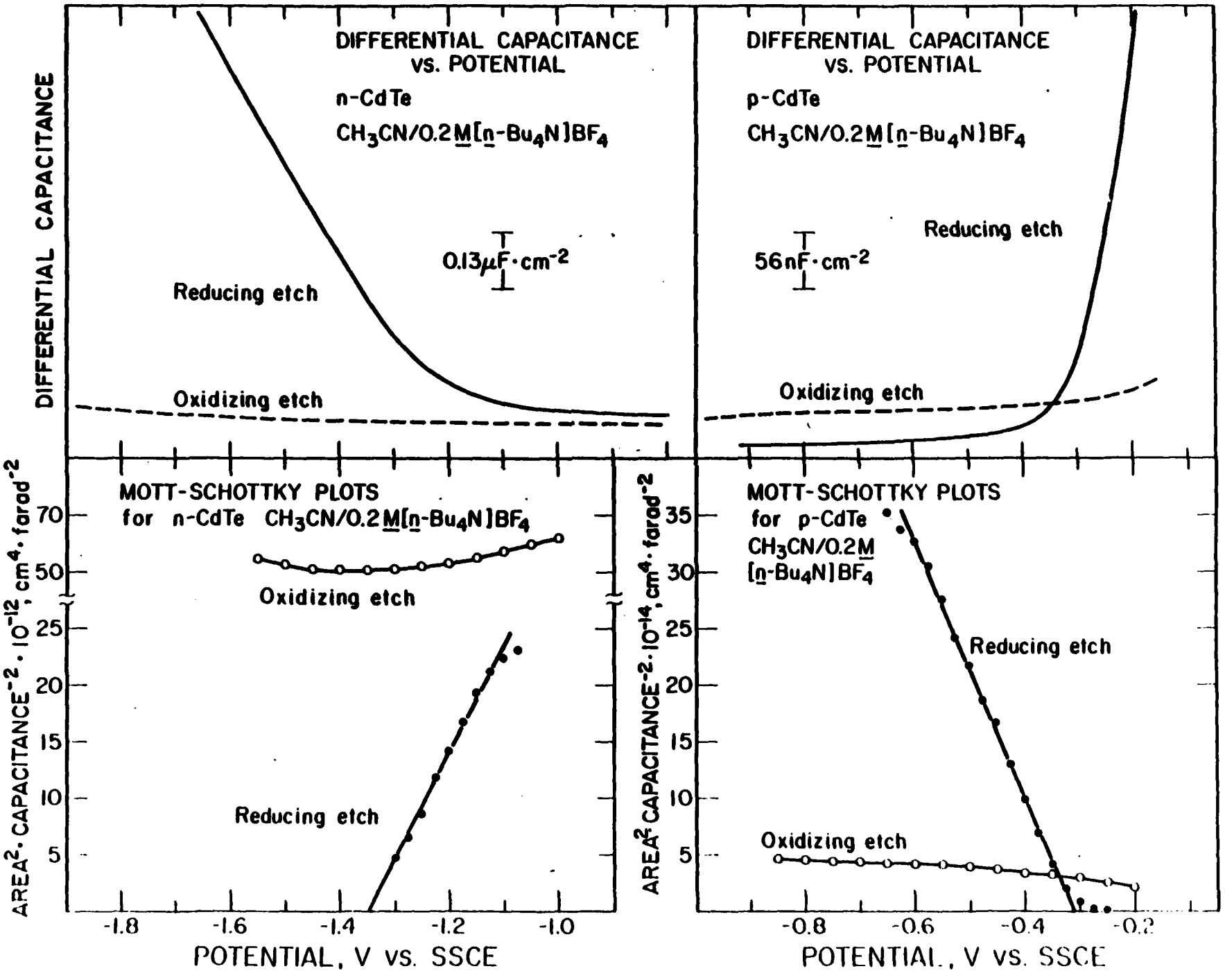
DIFFERENTIAL CAPACITANCE VS. POTENTIAL
n-CdTe
CH3CN/0.2M[n-Bu4N]BF4
0.13μF·cm-2
Reducing etch
Oxidizing etch
DIFFERENTIAL CAPACITANCE
DIFFERENTIAL CAPACITANCE VS. POTENTIAL
p-CdTe
CH3CN/0.2M[n-Bu4N]BF4
56nF·cm-2
Reducing etch
Oxidizing etch
MOTT-SCHOTTKY PLOTS
for n-CdTe CH3CN/0.2M[n-Bu4N]BF4
Oxidizing etch
Reducing etch
AREA2·CAPACITANCE-2·10-12, cm4·farad-2
70
50
25
20
15
10
5
-1.8
-1.6
-1.4
-1.2
-1.0
POTENTIAL, V vs. SSCE
MOTT-SCHOTTKY PLOTS
for p-CdTe
CH3CN/0.2M
[n-Bu4N]BF4
Reducing etch
Oxidizing etch
AREA2 CAPACITANCE-2·10-14, cm4·farad-2
35
30
25
20
15
10
5
-0.8
-0.6
-0.4
-0.2
POTENTIAL, V vs. SSCE

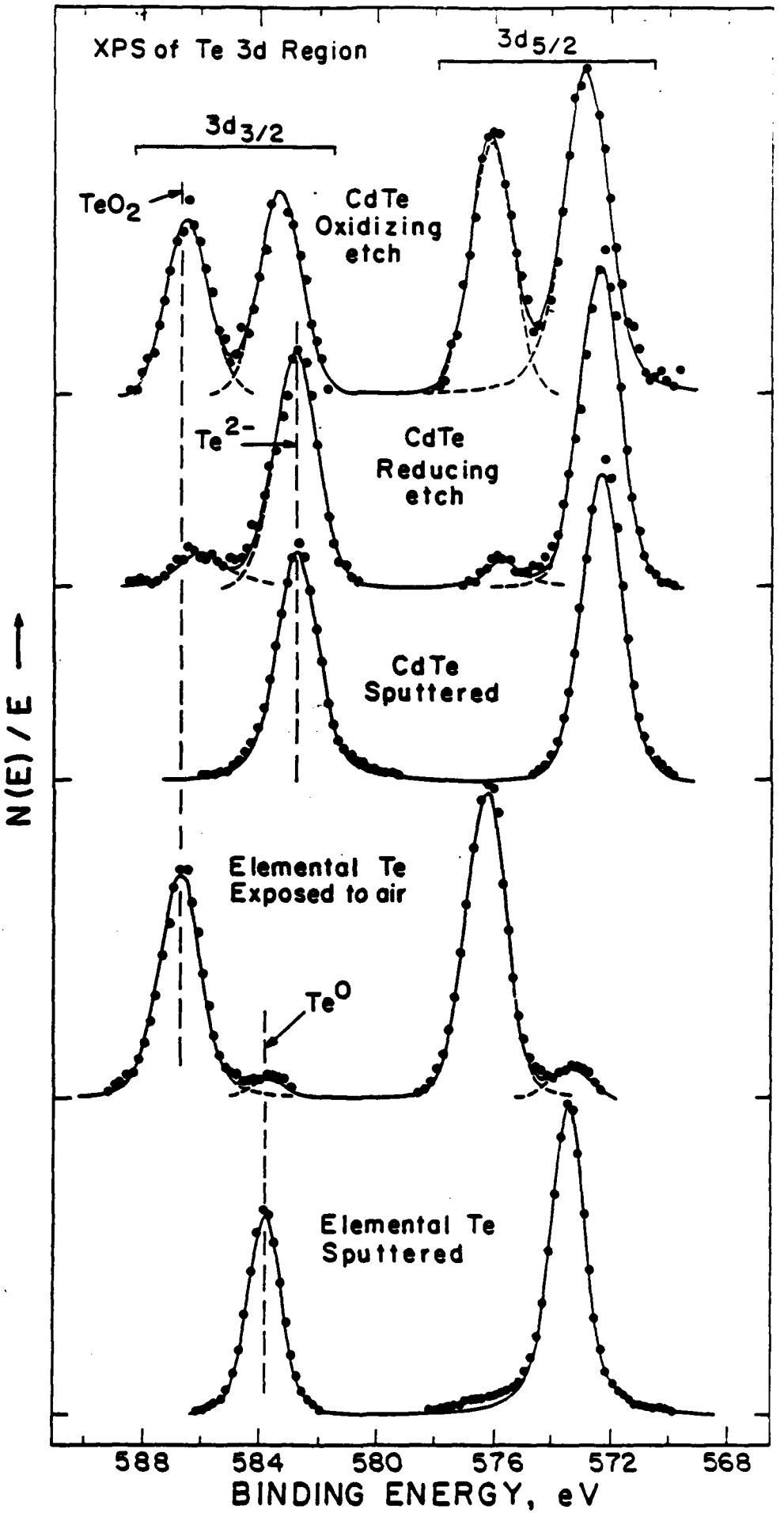
XPS of Te 3d Region
3d5/2
3d3/2
TeO2
CdTe
Oxidizing
etch
Te2-
CdTe
Reducing
etch
CdTe
Sputtered
Elemental Te
Exposed to air
Te0
Elemental Te
Sputtered
N(E) / E
588
584
580
576
572
568
BINDING ENERGY, eV

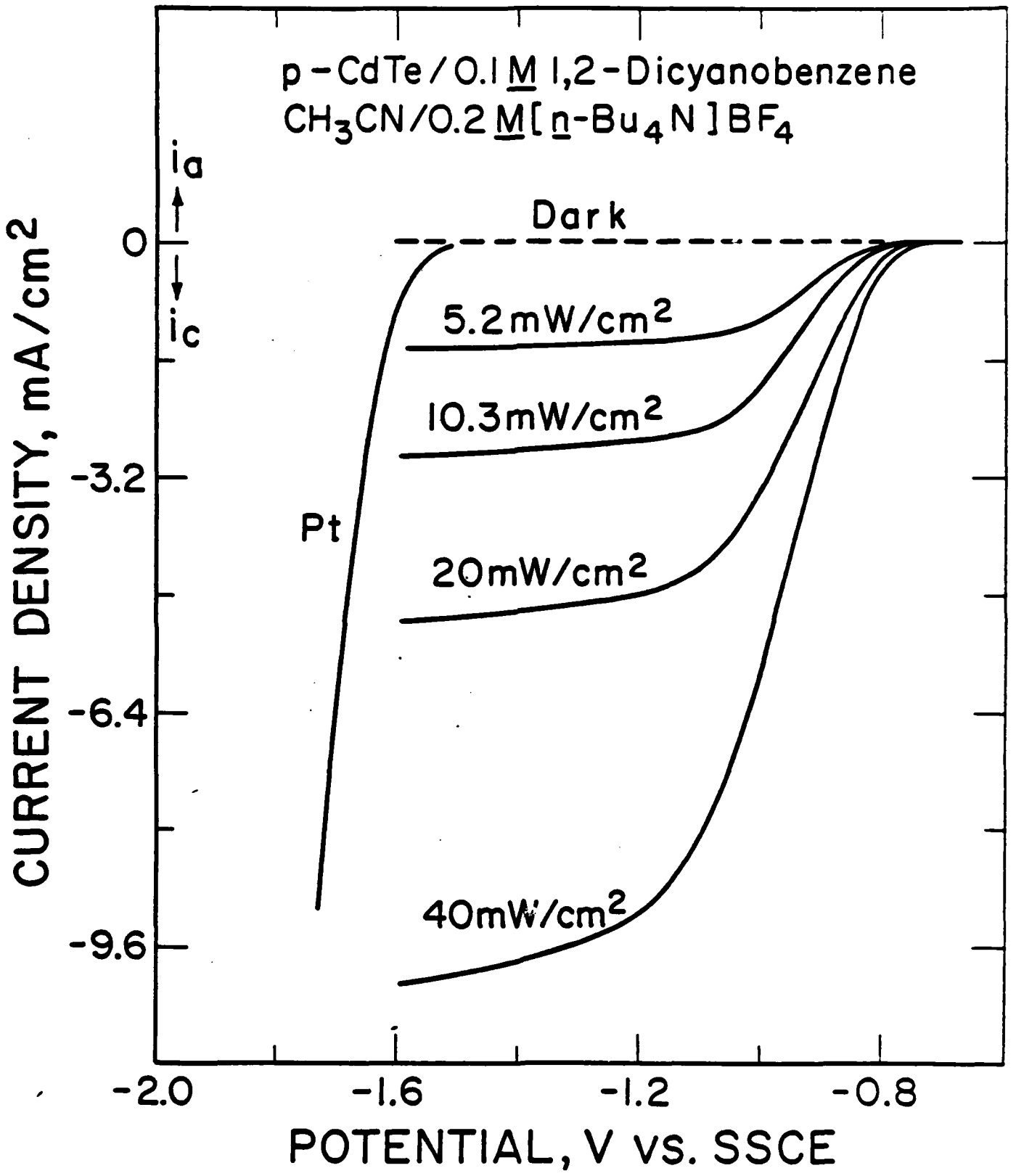
p-CdTe/0.1 M 1,2-Dicyanobenzene
CH3CN/0.2 M[n-Bu4N]BF4
ia
ic
Dark
5.2mW/cm2
10.3mW/cm2
20mW/cm2
40mW/cm2
Pt
0
-3.2
-6.4
-9.6
CURRENT DENSITY, mA/cm2
-2.0
-1.6
-1.2
-0.8
POTENTIAL, V vs. SSCE

472:GAN:716-4
94/GEN

TECHNICAL REPORT DISTRIBUTION LIST, GEN

	No. Copies
Office of Naval Research Attn: Code 413 800 North Quincy Street Arlington, Virginia 22217	2
ONR Pasadena Detachment Attn: Dr. R. J. Marcus 1030 East Green Street Pasadena, California 91106	1
Commander, Naval Air Systems Command Attn: Code 310C (H. Rosenwasser) Department of the Navy Washington, D.C. 20360	1
Defense Technical Information Center Building 5, Cameron Station Alexandria, Virginia 22314	12
Dr. Fred Saalfeld Chemistry Division, Code 6100 Naval Research Laboratory Washington, D.C. 20375	1
U.S. Army Research Office Attn: CRD-AA-IP P. O. Box 12211 Research Triangle Park, N.C. 27709	1
Mr. Vincent Schaper DTNSRDC Code 2803 Annapolis, Maryland 21402	1
Naval Ocean Systems Center Attn: Dr. S. Yamamoto Marine Sciences Division San Diego, California 91232	1
Naval Ocean Systems Center Attn: Mr. Joe McCartney San Diego, California 92152	1
Naval Weapons Center Attn: Dr. A. B. Amster, Chemistry Division China Lake, California 93555	1
Naval Civil Engineering Laboratory Attn: Dr. R. W. Drisko Port Hueneme, California 93401	1
Dean William Tolles Naval Postgraduate School Monterey, California 93940	1
Scientific Advisor Commandant of the Marine Corps (Code RD-1) Washington, D.C. 20380	1
Naval Ship Research and Development Center Attn: Dr. G. Bosmajian, Applied Chemistry Division Annapolis, Maryland 21401	1
Mr. John Boyle Materials Branch Naval Ship Engineering Center Philadelphia, Pennsylvania 19112	1
Mr. A. M. Anzalone Administrative Librarian PLASTEC/ARRADCOM Bldg 3401 Dover, New Jersey 07801	1

TECHNICAL REPORT DISTRIBUTION LIST, 051A

	No. Copies
Dr. M. A. El-Sayed Department of Chemistry University of California, Los Angeles Los Angeles, California 90024	1
Dr. E. R. Bernstein Department of Chemistry Colorado State University Fort Collins, Colorado 80521	1
Dr. C. A. Heller Naval Weapons Code 6059 China Lake, California 93555	1
Dr. J. R. MacDonald Chemistry Division Naval Research Laboratory Code 6110 Washington, D.C. 20375	1
Dr. G. B. Schuster Chemistry Department University of Illinois Urbana, Illinois 61801	1
Dr. A. Adamson Department of Chemistry University of Southern California Los Angeles, California 90007	1
Dr. M. S. Wrighton Department of Chemistry Massachusetts Institute of Technology Cambridge, Massachusetts 02139	1
Dr. A. Paul Schaap Department of Chemistry Wayne State University Detroit, Michigan 49207	1
Dr. M. Rauhut Chemical Research Division American Cyanamid Company Bound Brook, New Jersey 08805	1
Dr. J. I. Zink Department of Chemistry University of California, Los Angeles Los Angeles, California 90024	1
Dr. D. M. Burland IBM San Jose Research Center 5600 Cottle Road San Jose, California 95143	1
Dr. John Cooper Code 6130 Naval Research Laboratory Washington, D.C. 20375	1
Dr. William M Jackson Department of Chemistry Howard University Washington, D.C. 20059	1
Dr. George E. Walrafen Department of Chemistry Howard University Washington, D.C. 20059	1
Dr. Joe Brandelik AFWAL/AADO-1 Wright Patterson AFB Fairborn, Ohio 45433	1
Dr. Gary Bjorklund IBM 5600 Cottle Road San Jose, California 95143	1
Dr. Carmen Ortiz Cousejo Superior de Investigaciones Cientificas Serrano 117 Madrid 6, Spain	1

TECHNICAL REPORT DISTRIBUTION LIST, 359

	No. Copies
Dr. Paul Delahay Department of Chemistry New York University New York, New York 10003	1
Dr. E. Yeager Department of Chemistry Case Western Reserve University Cleveland, Ohio 41106	1
Dr. D. N. Bennion Department of Chemical Engineering Brigham Young University Provo, Utah 84602	1
Dr. R. A. Marcus Department of Chemistry California Institute of Technology Pasadena, California 91125	1
Dr. J. J. Auborn Bell Laboratories Murray Hill, New Jersey 07974	1
Dr. Adam Heller Bell Laboratories Murray Hill, New Jersey 07974	1
Dr. T. Katan Lockheed Missiles and Space Co., Inc. P. O. Box 504 Sunnyvale, California 94088	1
Dr. Joseph Singer, Code 302-1 NASA-Lewis 21000 Brookpark Road Cleveland, Ohio 44135	1
Dr. B. Brummer EIC Incorporated 55 Chapel Street Newton, Massachusetts 02158	1
Library P. R. Mallory and Company, Inc. Northwest Industrial Park Burlington, Massachusetts 01803	1
Dr. P. J. Hendra Department of Chemistry University of Southampton Southampton SO0 5NH United Kingdom	1
Dr. Sam Perone Chemistry & Materials Science Department Laurence Livermore National Lab. Livermore, California 94550	1
Dr. Royce W. Murray Department of Chemistry University of North Carolina Chapel Hill, North Carolina 27514	1
Naval Ocean Systems Center Attn: Technical Library San Diego, California 92152	1
Dr. C. E. Mueller The Electrochemistry Branch Materials Division, Research and Technology Department Naval Surface Weapons Center White Oak Laboratory Silver Spring, Maryland 20910	1
Dr. G. Goodman Johnson Controls 5757 North Green Bay Avenue Milwaukee, Wisconsin 53201	1
Dr. J. Boechler Electrochimica Corporation Attn: Technical Library 2485 Charleston Road Mountain View, California 94040	1
Dr. P. P. Schmidt Department of Chemistry Oakland University Rochester, Michigan 48063	1

TECHNICAL REPORT DISTRIBUTION LIST, 359

	No. Copies
Dr. H. Richtol Chemistry Department Rensselaer Polytechnic Institute Troy, New York 12181	1
Dr. A. B. Ellis Chemistry Department University of Wisconsin Madison, Wisconsin 53706	1
Dr. M. Wrighton Chemistry Department Massachusetts Institute of Technology Cambridge, Massachusetts 02139	
Larry E. Plew Naval Weapons Support Center Code 30736, Building 2906 Crane, Indiana 47522	1
S. Ruby DOE (STOR) 600 E Street Providence, Rhode Island 02192	1
Dr. Aaron Wold Brown University Department of Chemistry Providence, Rhode Island 02192	1
Dr. R. C. Chudacek McGraw-Edison Company Edison Battery Division Post Office Box 28 Bloomfield, New Jersey 07003	1
Dr. A. J. Bard University of Texas Department of Chemistry Austin, Texas 78712	1
Dr. M. M. Nicholson Electronics Research Center Rockwell International 3370 Miraloma Avenue Anaheim, California	1
Dr. R. P. Van Duyne Department of Chemistry Northwestern University Evanston, Illinois 60201	1
Dr. B. Stanley Pons Department of Chemistry University of Alberta Edmonton, Alberta CANADA T6G 2G2	1
Dr. Michael J. Weaver Department of Chemistry Michigan State University East Lansing, Michigan 48824	1
Dr. R. David Rauh EIC Corporation 55 Chapel Street Newton, Massachusetts 02158	1
Dr. J. David Margerum Research Laboratories Division Hughes Aircraft Company 3011 Malibu Canyon Road Malibu, California 90265	1
Dr. Martin Fleischmann Department of Chemistry University of Southampton Southampton 509 5NH England	1
Dr. Janet Osteryoung Department of Chemistry State University of New York at Buffalo Buffalo, New York 14214	1
Dr. R. A. Osteryoung Department of Chemistry State University of New York at Buffalo Buffalo, New York 14214	1

TECHNICAL REPORT DISTRIBUTION LIST, 359

	No. Copies
Dr. Donald W. Ernst Naval Surface Weapons Center Code R-33 White Oak Laboratory Silver Spring, Maryland 20910	1
Dr. R. Nowak Naval Research Laboratory Code 6130 Washington, D.C. 20375	1
Dr. John F. Houlihan Shenango Valley Campus Pennsylvania State University Sharon, Pennsylvania 16146	1
Dr. D. F. Shriver Department of Chemistry Northwestern University Evanston, Illinois 60201	1
Dr. D. H. Whitmore Department of Materials Science Northwestern University Evanston, Illinois 60201	1
Dr. Alan Bewick Department of Chemistry The University Southampton, S09 5NH England	
Dr. A. Himy NAVSEA-5433 NC #4 2541 Jefferson Davis Highway Arlington, Virginia 20362	
Dr. John Kincaid Department of the Navy Strategic Systems Project Office Room 901 Washington, D.C. 20376	
Mr. James R. Moden Naval Underwater Systems Center Code 3632 Newport, Rhode Island 02840	1
Dr. Bernard Spielvogel U. S. Army Research Office P. O. Box 12211 Research Triangle Park, NC 27709	1
Dr. Denton Elliott Air Force Office of Scientific Research Bolling AFB Washington, D.C. 20332	1
Dr. David Aikens Chemistry Department Rensselaer Polytechnic Institute Troy, New York 12181	1
Dr. A. P. B. Lever Chemistry Department York University Downsview, Ontario M3J1P3 Canada	1
Dr. Stanislaw Szpak Naval Ocean Systems Center Code 6343 San Diego, California 95152	1
Dr. Gregory Farrington Department of Materials Science and Engineering University of Pennsylvania Philadelphia, Pennsylvania 19104	
Dr. Bruce Dunn Department of Engineering & Applied Science University of California Los Angeles, California 90024	

TECHNICAL REPORT DISTRIBUTION LIST, 359

	No. Copies
M. L. Robertson Manager, Electrochemical and Power Sonices Division Naval Weapons Support Center Crane, Indiana 47522	1
Dr. Elton Cairns Energy & Environment Division Lawrence Berkeley Laboratory University of California Berkeley, California 94720	1
Dr. Micha Tomkiewicz Department of Physics Brooklyn College Brooklyn, New York 11210	1
Dr. Lesser Blum Department of Physics University of Puerto Rico Rio Piedras, Puerto Rico 00931	1
Dr. Joseph Gordon, II IBM Corporation K33/281 5600 Cottle Road San Jose, California 95193	1
Dr. Robert Somoano Jet Propulsion Laboratory California Institute of Technology Pasadena, California 91103	1
Dr. Johann A. Joebstl USA Mobility Equipment R&D Command DRDME-EC Fort Belvior, Virginia 22060	1
Dr. Judith H. Ambrus NASA Headquarters M.S. RTS-6 Washington, D.C. 20546	1
Dr. Albert R. Landgrebe U.S. Department of Energy M.S. 6B025 Forrestal Building Washington, D.C. 20595	1
Dr. T. Marks Department of Chemistry Northwestern University Evanston, Illinois 60201	1
Dr. D. Cipris Allied Corporation P. O. Box 3000R Morristown, New Jersey 07960	1
Dr. M. Philpot IBM Corporation 5600 Cottle Road San Jose, California 95193	1
Dr. Donald Sandstrom Washington State University Department of Physics Pullman, Washington 99164	1
Dr. Carl Kannewurf Northwestern University Department of Electrical Engineering and Computer Science Evanston, Illinois 60201	1
Dr. Edward Fletcher University of Minnesota Department of Mechanical Engineering Minneapolis, Minnesota 55455	1
Dr. John Fontanella U.S. Naval Academy Department of Physics Annapolis, Maryland 21402	1
Dr. Martha Greenblatt Rutgers University Department of Chemistry New Brunswick, New Jersey 08903	1
Dr. John Wassib Kings Mountain Specialties P. O. Box 1173 Kings Mountain, North Carolina 28086	1

TECHNICAL REPORT DISTRIBUTION LIST, 359

	No. Copies	No. Copies
Dr. J. J. Brophy University of Utah Department of Physics Salt Lake City, Utah 84112	1	
Dr. Walter Roth Department of Physics State University of New York Albany, New York 12222	1	
Dr. Thomas Davis National Bureau of Standards Polymer Science and Standards Division Washington, D.C. 20234	1	
Dr. Charles Martin Department of Chemistry Texas A&M University	1	
Dr. Anthony Sammells Institute of Gas Technology 3424 South State Street Chicago, Illinois 60616	1	
Dr. H. Tachikawa Department of Chemistry Jackson State University Jackson, Mississippi 39217	1	
Dr. W. M. Risen Department of Chemistry Brown University Providence, Rhode Island	1	

END

FILMED

9-83

DTIC